

1 **Title Page**

2
3 **Impact of Pulmonary Endarterectomy on Pulmonary Arterial Wave Propagation**
4 **and Reservoir Function**

5
6 Running title: WIA and Reservoir Function Pre- and Post-PEA

7 Word count: 9028 Main text: 4969

8 Figures and tables: 9

9
10 Junjing Su^{1,2}, Alun D Hughes^{2,3}, Ulf Simonsen¹, Jens Erik Nielsen-Kudsk⁴, Kim H
11 Parker⁵, *Luke S Howard¹, *Soren Mellekjaer⁴ (*Equal contribution)

12
13 ¹Department of Biomedicine, Aarhus University; ²National Heart and Lung Institute,
14 Imperial College London; ³Institute of Cardiovascular Science, University College
15 London; ⁴Department of Cardiology, Aarhus University Hospital; ⁵Department of
16 Bioengineering, Imperial College London

17
18 **Correspondence:**

19 Junjing Su, PhD, Department of Biomedicine – Pharmacology, Aarhus University,
20 Wilhelm Meyers Allé 4, 8000 Aarhus C, Denmark
21 Email: junjing.su@biomed.au.dk
22 Tel + 45 8716 7692 Fax +45 8715 0201

26 **Abstract**

27

28 High wave speed and large wave reflection in the pulmonary artery have previously
29 been reported in patients with chronic thromboembolic pulmonary hypertension
30 (CTEPH). We assessed the impact of pulmonary endarterectomy (PEA) on pulmonary
31 arterial wave propagation and reservoir function in CTEPH patients. Right heart
32 catheterization was performed using a combined pressure and Doppler flow sensor
33 tipped guidewire to obtain simultaneous pressure and flow velocity measurements in the
34 pulmonary artery in eight CTEPH patients before and 3 months after PEA. Wave
35 intensity and reservoir-excess pressure analyses were then performed. Following PEA,
36 mean pulmonary arterial pressure (PAPm, ~49 versus ~32 mmHg), pulmonary vascular
37 resistance (PVR, ~11.1 versus ~5.1 Wood Units) and wave speed (~16.5 versus ~8.1
38 m/s), i.e. local arterial stiffness, markedly decreased. The changes in the intensity of the
39 reflected arterial wave and wave reflection index (pre: ~28%; post: ~22%) were small
40 and post-PEA patients with and without residual pulmonary hypertension (i.e. PAPm
41 \geq 25 mmHg) had similar wave reflection index (~20 versus ~23%). The reservoir and
42 excess pressure decreased post-PEA and the changes were associated with improved
43 right ventricular afterload, function and size. In conclusion, while PVR and arterial
44 stiffness decreased substantially following PEA, large wave reflection persisted, even in
45 patients without residual pulmonary hypertension, indicating lack of improvement in
46 vascular impedance mismatch. This may continue to affect the optimal ventriculo-
47 arterial interaction and further studies are warranted to determine whether this
48 contributes to persistent symptoms in some patients.

49

50 **Keywords:** pulmonary hypertension, pulmonary endarterectomy, wave intensity
51 analysis, wave reflection, arterial stiffness

52

53 **New and Noteworthy**

54

55 We performed wave intensity analysis in the pulmonary artery in patients with chronic
56 thromboembolic pulmonary hypertension before and 3 months after pulmonary
57 endarterectomy. Despite of substantial reduction in pulmonary arterial pressures,
58 vascular resistance and arterial stiffness, large pulmonary arterial wave reflection
59 persisted 3 months post-surgery, even in patients without residual pulmonary
60 hypertension, suggestive of lack of improvement in vascular impedance mismatch.

61

62

63

64 **Introduction**

65

66 Chronic thromboembolic pulmonary hypertension (CTEPH) is characterized by an
67 elevated mean pulmonary arterial pressure (PAPm) ≥ 25 mmHg due to obstruction of
68 the pulmonary arteries following an episode or recurrent episodes of pulmonary
69 embolism (16). Left untreated, the disease progresses to right heart failure and death.
70 The treatment of choice is pulmonary endarterectomy (PEA), which has dramatically
71 increased the survival of CTEPH patients (15). However, despite technically successful
72 endarterectomy, some patients remain symptomatic (6). Current hemodynamic
73 evaluation of pulmonary hypertension (PH) mainly focusses on PAPm and pulmonary
74 vascular resistance (PVR), i.e. the steady component of right ventricular (RV) afterload,
75 while the pulsatile (dynamic) afterload, which is related to arterial stiffness and wave
76 reflection, is often neglected.

77 Wave intensity analysis (WIA) is a time-domain based approach for the assessment
78 of pulsatile afterload and ventricular function. It quantifies the intensity, origin, type and
79 timing of arterial waves (41, 51). Forward traveling waves arise from ventricular
80 contraction or relaxation, which generate forward compression (FCW) or
81 decompression waves (FDW) that increase or decrease pressure and flow, respectively.
82 Backward traveling waves, e.g. reflected waves, originate as a consequence of
83 admittance (or inversely impedance) mismatching in the vasculature. Depending on the
84 nature of the admittance mismatch, they can be backward compression waves (BCW)
85 that increase the pressure while decreasing the flow or backward decompression waves
86 that decrease the pressure while increasing the flow. In addition to characterizing wave
87 intensity, direction and type, WIA can also be used to determine wave speed (i.e. local
88 pulse wave velocity), a measure of arterial stiffness. Previous studies applying WIA in

89 the pulmonary artery have revealed distinctive wave characteristics in CTEPH patients.
90 Notably, greater wave speed and wave reflection were observed indicative of increased
91 local arterial stiffness and admittance mismatching between the proximal and distal
92 vasculature, respectively (44, 52).

93 Another approach that can be used to describe the arterial system is the reservoir-
94 excess pressure analysis (40, 59), which characterizes the measured pressure waveform
95 in terms of a reservoir and excess pressure and is, to some extent, analogous to the 3-
96 element Windkessel model of the circulation (58). The application of reservoir-excess
97 pressure analysis is increasingly being used in the systemic circulation and indices
98 derived from the analysis have been shown to predict cardiovascular events (12, 20, 38).
99 However, only a limited number of studies have explored the reservoir-excess pressure
100 approach in the pulmonary artery (18, 53) and these have shown increased reservoir and
101 excess pressures in PH patients.

102 The influence of PEA on pulmonary arterial wave propagation and reservoir function
103 has not been investigated previously and here, we use WIA and reservoir-excess
104 pressure analysis to provide additional information about the RV load and pulmonary
105 vasculature following PEA.

106

107 **Methods**

108

109 **Ethical Approval**

110

111 Study participants were selected among patients undergoing clinical investigations
112 for CTEPH at Hammersmith Hospital, Imperial College Healthcare, United Kingdom,
113 and Aarhus University Hospital, Denmark. Patient inclusion criteria were standardized

114 and an identical protocol was used at both centers to avoid bias. The same investigator
115 (JS) collected all the data at both sites to avoid inter-observer variability. Patients were
116 excluded if CTEPH was ruled out or if they were considered unsuitable for PEA, which
117 was performed either at Papworth Hospital, Cambridge or Aarhus University Hospital.
118 The study complied with the Declaration of Helsinki and was approved by the local
119 Ethics Committees (references 13/LO/1305 and M-2013-278-13) and all participants
120 gave written informed consent.

121

122 **Study Protocol**

123

124 Right heart catheterization was performed using a 6 Fr balloon flotation catheter that
125 was advanced into the pulmonary artery via the right brachial or jugular vein.
126 Subsequently, a combined dual-tipped pressure and Doppler flow sensor wire
127 (Combwire, Philips Volcano, California, USA) was advanced approximately 1 cm
128 beyond the end of the catheter (52). Doppler flow velocity signals were optimized by
129 careful manipulation of the catheter and wire *in situ*. Once stable signals were observed,
130 pressure and velocity data were acquired simultaneously at a sampling rate of 200 Hz
131 for ~60 seconds together with ECG monitoring in a free breathing state in the main, left
132 and right pulmonary arteries (PA). All patients were in sinus rhythm at the time of
133 investigation. All investigations including routine transthoracic echocardiography and
134 blood tests were performed before and 3 months after PEA. In addition to the included
135 CTEPH patients, analyses were also applied to the acquired pressure and velocity data
136 from the pulmonary arteries of patients without pulmonary vascular disease that were
137 included in a previous study and these patients served as controls (52).

138

139 **Right Ventricular Work and Afterload**

140

141 The global pulmonary arterial compliance was calculated as right ventricular stroke
142 volume (RVSV) divided by pulmonary arterial pulse pressure. PVR was calculated as
143 the transpulmonary pressure difference, defined as the difference between PAPm and
144 pulmonary arterial wedge pressure (PAWP), divided by cardiac output. Total
145 pulmonary resistance (TPR) was calculated as PAPm divided by cardiac output.

146 RV power and energy densities, defined as the power and energy , respectively,
147 delivered by the right ventricle to generate the stroke volume per unit cross sectional
148 area (CSA) of the artery, are useful dimensions for comparison with wave intensity (i.e.
149 power density) and energy density. Given the heart rate (HR) and mean flow velocity
150 (U_{mean}), RV power/energy densities were derived from steady flow RV stroke work
151 (RVSW) (8) using previously described formulas (Equations 1 – 3) (52).

152 (1)
$$RV\ energy\ density = \frac{RVSW}{CSA} = \frac{(PAPm - RAP) \cdot RVSV}{RVSV \cdot HR / U_{mean}} = \frac{(PAPm - RAP)}{HR / U_{mean}}$$

153 Hence,

154 (2)
$$RV\ energy\ density = (PAPm - RAP) \cdot U_{mean} \cdot CCD$$

155 and

156 (3)
$$RV\ power\ density = (PAPm - RAP) \cdot U_{mean}$$

157 where RAP is the right atrial pressure and CCD is the duration of the cardiac cycle.

158

159 **Wave Intensity Analysis**

160

161 Recorded pressure (P) and velocity (U) data were processed offline using customized
162 Matlab software (v2015a MathWorks, Massachusetts, USA). Using the R-wave on ECG
163 as a fiducial marker, pressure and velocity signals were ensemble-averaged and

164 smoothed using a Savitzky-Golay differentiating filter (2nd order polynomial fit,
 165 window size 11). Hardware-related delay between pressure and velocity signals was
 166 corrected by shifting the velocity data until the beginning of the upslope of the velocity
 167 and pressure waveforms were aligned (52).

168 The wave speed (c) was calculated using the sum of squares method (Equation 4)
 169 (13).

$$170 \quad (4) \quad c = \frac{1}{\rho} \cdot \sqrt{\frac{\sum dP^2}{\sum dU^2}}$$

171

172 Where ρ is the blood density, assumed to be 1040 kg/m³ and the summation was taken
 173 over the entire cardiac period.

174 Another common approach to determine the local wave speed is the PU-loop method,
 175 where pressure is plotted against velocity and the slope of the early linear portion of the
 176 PU-curve is expected to be equal to the product of blood density and wave speed (24).
 177 This is only valid under the assumption that there is no wave reflection in early systole,
 178 i.e. that there is an early linear segment. However, in many of our subjects, the PU-loop
 179 did not display a linear initial segment and in practice, PU-loop estimates of wave speed
 180 were poorly reproducible; therefore, we chose to use the sum of squares method.

181 Wave intensity was separated into its forward (WI_+) and backward (WI_-) components
 182 and normalized to the duration of the cardiac cycle (CCD) to make it independent of
 183 sampling rate (52, 53) (Equation 5).

$$184 \quad (5) \quad WI_{\pm} = \pm \left(\frac{dP \cdot CCD}{dt} \pm \rho c \cdot \frac{dU \cdot CCD}{dt} \right)^2 / (4\rho c)$$

185

186 Separated waves were quantified by the peak intensity of the individual waves
 187 (W/m²) and by the cumulative area under each wave (J/m²) corresponding to the power

188 and energy, respectively, carried by each wave per cross sectional area of the artery over
 189 a cardiac cycle squared. Wave reflection index (WRI) was calculated as the ratio of the
 190 BCW to FCW energy.

191

192 ***Reservoir-excess Pressure Analysis***

193

194 The reservoir-excess pressure approach was originally developed using both pressure
 195 and flow velocity data (59). However, as flow velocity is rarely measured during
 196 clinical settings, here, reservoir-excess pressure analysis was performed using only the
 197 measured pressure (Equation 6) (2), as this method can be reproduced by most
 198 investigators. Both methods give quantitatively similar results.

199

200 (6)

201 $P_r =$

$$202 P_0 \cdot e^{-(k_s+k_d)t} + P_\infty \frac{k_d}{k_s+k_d} (1 - e^{-(k_s+k_d)t}) + k_s \cdot e^{-(k_s+k_d)t} \int_0^t P(t') e^{-(k_s+k_d)t'} dt'$$

203

204

205 The reservoir pressure (P_r) varies in magnitude through changes in the resistance (R) to
 206 outflow from the reservoir, the reservoir compliance (C) and the asymptotic pressure
 207 (P_∞), which is the limit for the exponential decay of the reservoir pressure during
 208 diastole and corresponds to the pressure at which outflow through the microcirculation
 209 would be predicted to be zero assuming a mono-exponential decay (Figure 1). k_s is the
 210 rate constant for reservoir filling. It is the inverse of the product of compliance and the
 211 ratio between arterial inflow and excess pressure. This ratio is related to, but not
 212 necessarily equal to, the characteristic impedance of the pulmonary artery (by analogy

213 with the 3-element Windkessel model). k_d is the constant for reservoir emptying. P_0 is
214 the pressure at time, t_0 , corresponding to the end of ventricular ejection, i.e. at the time
215 of closure of the pulmonary valve (Figure 1). This was assumed to correspond to the
216 time of maximal negative dP/dt (1, 45). The excess pressure (P_x) is calculated as the
217 difference between the measured pressure and the reservoir pressure.

218 Reservoir and excess pressures were quantified by peak P_r (minus diastolic pressure)
219 and P_x , and the integral of P_r (minus diastolic pressure) and P_x , respectively. Note that
220 WIA described above was applied to the measured pressure rather than the calculated
221 excess pressure, as the validity of WIA using the excess pressure remains controversial
222 (37, 49).

223 Three different estimates of the diastolic pressure decay time were calculated. The
224 diastolic time constant, τ , i.e. the inverse of the k_d , was derived from the reservoir-
225 excess pressure analysis. The RC-time was calculated as RC_{PVR} , defined as the product
226 of PVR and arterial compliance (C_p) (56) and RC_{TPR} , defined as the product of TPR and
227 C_p (27).

228

229 **Statistical Analysis**

230

231 Sample data are summarized as means \pm SD. Differences between pre- and post-PEA
232 data were then compared using a paired Student's t-test. WIA and reservoir parameters
233 from the main, right and left PAs were analyzed using mixed linear models to examine
234 the differences between pre- and post-PEA data. These data are presented as estimated
235 marginal means and 95 % CI. Where appropriate, data were log-transformed prior to
236 analysis to achieve normally distributed residuals. 1-way repeated measures analysis of
237 variance (ANOVA) was performed to detect differences between τ , RC_{PVR} and RC_{TPR} .

238 Post-hoc tests following ANOVA employed a Bonferroni adjustment for multiple
239 testing. Spearman's correlation analysis was performed to examine monotonic
240 relationships between variables. Following PEA, the patients were separated into two
241 groups *a priori*: those with residual PH and those without (i.e. a PAPm < 25 mmHg
242 after surgery). Differences in WIA and reservoir parameters between the two groups
243 and controls were compared using mixed linear models. The level of significance was
244 set at $p < 0.05$. All statistical analyses were performed using Stata (v13, StataCorp,
245 Texas, USA).

246

247 **Results**

248

249 **Patient Characteristics**

250

251 In total, 10 CTEPH patients underwent PEA. Two patients were lost to follow-up
252 and the remaining eight patients (67 ± 9 years, 3 male) completed the post-PEA
253 investigations. Average waiting period from the initial assessment to PEA was 4.0 ± 2.3
254 months and average time to first follow-up post-PEA was 3.8 ± 1.1 months. Significant
255 symptomatic and hemodynamic improvements were achieved following PEA (Table 1).
256 Overall, PAPm decreased by 16 ± 17 mmHg, PVR decreased by 6.0 ± 5 Wood Units
257 and cardiac output increased by 1.3 ± 1.1 l/min (Table 1 and Supplementary Figure S1:
258 https://osf.io/h2dwk/?view_only=765df6c79dcf4d4ab9c697be0c4701ae). RV size
259 reduced and RV function improved (Supplementary Table S1:
260 https://osf.io/h2dwk/?view_only=765df6c79dcf4d4ab9c697be0c4701ae).

261 PAPm dropped to <25 mmHg in three patients (out of 8) following PEA. These
262 patients also had a significantly smaller right atrium and ventricle post-PEA compared

263 to patients with residual PH (defined as PAPm \geq 25 mmHg, data not shown). In two
264 patients, PAPm increased after PEA; in one of them the increased PAPm could be
265 explained by increased cardiac output. The cardiac output remained the same in one
266 patient and increased in the rest of the cohort (Supplementary Figure S1:
267 https://osf.io/h2dwk/?view_only=765df6c79dcf4d4ab9c697be0c4701ae). Post-PEA
268 hemodynamic outcomes did not appear to be associated with pre-operative
269 hemodynamic measurements, RV size or function, and was unrelated to whether the
270 patient had predominantly main/lobar or segmental artery disease.

271

272 **Arterial Wave Characteristics**

273

274 The pressure and flow velocity profiles and the corresponding WIA patterns from the
275 main pulmonary artery of a patient before (Figure 2A & B) and after (Figure 2C & D)
276 surgery are shown. This patient achieved a substantial drop in pulmonary pressures with
277 a PAPm <25 mmHg post-PEA along with a substantial increase in flow velocity. WIA
278 revealed three dominant systolic waves. The observed FCW in early systole and FDW
279 in late systole were generated by RV contraction and relaxation, respectively, while the
280 mid-systolic BCW was attributed to reflection of the preceding FCW. Following PEA,
281 BCW did not diminish. For comparison, WIA pattern of a representative control subject
282 (Figure 2E & F) without pulmonary vascular disease from a previous study (52) showed
283 minimal BCW. Table 2 shows the estimated marginal means of the pooled WIA indices
284 from the three PA branches (summary statistics for each of the branch are shown in
285 Supplementary Table S2:

286 https://osf.io/h2dwk/?view_only=765df6c79dcf4d4ab9c697be0c4701ae). Following
287 PEA, wave speed significantly decreased by 8 m/s [95 % CI: 6; 11 m/s]. The intensity

288 of BCW and wave reflection index (WRI, defined as the ratio between BCW and FCW
289 energy) also decreased, although the decrease in WRI (by 6 % [95 % CI: 1 ; 13 %]) did
290 not achieve statistical significance. FCW intensity and energy density and the ratio of
291 FCW to RV stroke power and energy densities remained essentially unchanged.

292 When compared to control subjects without pulmonary vascular disease (N = 10, 59
293 \pm 14 years, 8 male) from our previous study (52), post-PEA wave speed and wave
294 energy were much greater in patients with residual PH (Figure 3). Patients that achieved
295 a PAPm <25 mmHg post-PEA had significantly lower wave speed than those with
296 residual PH, although it remained significantly greater compared to controls. In
297 contrast, post-PEA WRI in patients with a PAPm <25 mmHg was similar to patients
298 with residual PH and it remained substantially greater than individuals without
299 pulmonary vascular disease (Figure 3C).

300

301 **Reservoir Function**

302

303 Separation of the measured pressure into a reservoir pressure and an excess pressure
304 is illustrated in Figure 4. Table 3 shows the estimated marginal means of the pooled
305 reservoir indices from the three PA branches (summary statistics for each of the branch
306 are shown in Supplementary Table S3:

307 https://osf.io/h2dwk/?view_only=765df6c79dcf4d4ab9c697be0c4701ae). Both the

308 reservoir and excess pressures decreased following PEA (Table 3, Figure 4C & D).

309 Comparison of the morphology of the excess pressure waveform with the velocity
310 waveform in patients with CTEPH showed that the two waveforms deviated from one
311 another noticeably in mid-systole (Figure 4B & D) consistent with substantial wave
312 reflection. This was not seen in controls (Figure 4F). The morphology of the flow

313 velocity waveform was also noticeably different in patients with CTEPH (before and
314 after PEA) compared with controls (compare 4B, D & F).

315 Compared to control subjects without pulmonary vascular disease and patients
316 without residual PH post-PEA, the reservoir, excess and asymptotic pressures were
317 significantly greater in patients with residual PH (Figure 5). However, patients without
318 residual PH post-PEA had a reservoir pressure (both peak and integral) that remained
319 significantly greater compared to controls (Figure 5A). Post-PEA excess pressure of
320 patients without residual PH was also greater compared to controls; while there was a
321 large degree of normalization of the asymptotic pressure (Figure 5B and 5C).

322 Estimates of the diastolic pressure decay time, using the parameters τ , RC_{PVR} and
323 RC_{TPR} , differed significantly from each other both pre and post-PEA. Expectedly, there
324 was a strong correlation between RC_{PVR} and RC_{TPR} , while post-PEA τ was moderately
325 correlated to RC_{PVR} and RC_{TPR} (Figure 6). PEA did not affect RC_{TPR} (Table 3). In
326 contrast, τ increased and RC_{PVR} reduced following PEA. Of note, post-PEA (but not
327 pre-PEA) τ was significantly correlated to the post-PEA asymptotic pressure.

328

329 **Correlation Analyses**

330

331 The correlation of changes (post-PEA minus pre-PEA values) in the WIA and
332 reservoir indices from the main pulmonary artery to the conventionally used
333 hemodynamic measurements, echocardiographic parameters reflecting RV size and
334 function and B-type natriuretic peptide (BNP) was examined (Supplementary Table S4:
335 https://osf.io/h2dwk/?view_only=765df6c79dcf4d4ab9c697be0c4701ae). Decreased
336 wave speed was significantly correlated to changes in PVR ($\rho = 0.79$, $p = 0.02$),
337 arterial compliance ($\rho = -0.81$, $p = 0.01$) and BNP ($\rho = 0.82$, $p = 0.02$). The decrease

in reservoir pressure was significantly associated with the decrease in pulse pressure ($\rho = 0.98$, $p < 0.01$) and the increase in arterial compliance ($\rho = -0.88$, $p < 0.01$) and decreased excess pressure was significantly correlated to decreased RV diastolic diameter ($\rho = 0.79$, $p = 0.02$), RV area ($\rho = 0.74$, $p = 0.04$) and decreased BNP ($\rho = 0.82$, $p = 0.02$). Decreased asymptotic pressure was significantly associated with decreased PAPm ($\rho = 0.95$, $p < 0.01$) and decreased PVR ($\rho = 0.79$, $p = 0.02$). In contrast, changes in wave energy and WRI were not significantly correlated to changes in any of the conventionally used hemodynamic parameters or RV size and function (Supplementary Table S4: https://osf.io/h2dwk/?view_only=765df6c79dcf4d4ab9c697be0c4701ae), although there was a moderate positive correlation between the decrease in FCW energy and decreased BNP ($\rho = 0.71$; $p = 0.07$).

Discussion

We used WIA and reservoir-excess pressure analysis to assess the influence of PEA on pulmonary arterial wave propagation and reservoir function. Following PEA, PAPm decreased (it was below 25 mmHg in more than 1/3 of the patients). The local wave speed also decreased markedly, but wave reflection was only slightly reduced, even in patients with a PAPm < 25 mmHg post-PEA. Reservoir, excess and asymptotic pressures all decreased and these changes were associated with improved RV afterload, function and size; Finally, RC_{PVR} decreased and τ increased, while RC_{TPR} appeared to be unchanged.

Impact of PEA on Wave Speed and Wave Energy

363

364 Consistent with previous studies (11, 17), significant improvements in pulmonary
365 hemodynamics and RV function were observed 3 months post-PEA with ~34 %
366 reduction in PAPm, ~55 % reduction in PVR and ~32 % increase in cardiac output.
367 Corresponding to improved arterial compliance, wave speed, a measure of pulmonary
368 arterial stiffness, decreased by ~50 %; although, it remained significantly higher than
369 the wave speed of control subjects, even in patients with a PAPm < 25 mmHg after
370 surgery. The contribution of arterial stiffness to RV afterload is often neglected;
371 however, its inverse, arterial compliance, has been shown to be a strong independent
372 predictor of mortality in pulmonary arterial hypertension patients (32, 33), and in the
373 systemic circulation, aortic pulse wave velocity is an independent predictor of
374 cardiovascular events (5, 29).

375 FCW energy represents the work done by the ventricle to generate pulse waves,
376 while RV stroke work accounts for the energy used to maintain steady flow; both
377 remained essentially unchanged after PEA, although there was some evidence of
378 normalization in patients with a PAPm < 25 mmHg after surgery. The ratio of FCW to
379 RV stroke work also remained unchanged indicating unaffected proportional
380 contribution of the wave and mean power to the total RV hydraulic power. FCW is
381 generated during RV ejection and consequently, its magnitude is influenced by RV
382 preload, contractility and the properties of the pulmonary artery (23). The preserved
383 wave energy and RV stroke work may therefore be explained by the increased cardiac
384 output post-PEA due to decreased RV afterload.

385

386 **Impact of PEA on Wave Reflection**

387

388 Reflected waves are generated when the energy transmission property between the
389 proximal and distal vasculature differs leading to an admittance (or inversely
390 impedance) mismatch (41). Reflected compression waves that arrive in systole augment
391 pressure and impede flow and therefore constitute an additional load on the contracting
392 right ventricle. The normal pulmonary circulation is efficiently constructed so that it
393 facilitates forward traveling waves and impedes backward traveling waves (60), while
394 high intensity reflected waves are evident in CTEPH patients (44, 52). Interestingly,
395 high intensity reflected waves were observed both pre- and post-PEA and the magnitude
396 of wave reflection diminished only slightly following PEA. In a previous study, we
397 have demonstrated that large wave reflection was present in patients with mildly
398 elevated pulmonary pressures, similar to those with severely elevated pulmonary
399 pressures and thus, we suggested that vascular impedance mismatch may occur in the
400 initial phase of pulmonary vascular disease (52). In keeping with these previous
401 observations, the findings from the present study suggest that despite substantial
402 reduction in pulmonary pressures and PVR in some patients, some degree of vascular
403 admittance mismatch persisted. This may be indicative of residual pulmonary arterial
404 disease, which may continue to adversely affect interactions between the right ventricle
405 and the vasculature. Persistent large wave reflection post-PEA does not imply that
406 removal of thrombi did not influence wave energy transmission. Wave behavior in the
407 vicinity of thrombi is poorly understood. Thrombi may act as a reflector or they may
408 partially absorb energy. Although the net wave reflection remained large, it is difficult
409 to establish whether the location of the reflection sites altered. Some studies (28, 44)
410 have used the local wave speed and half of the time difference between FCW to BCW
411 to give an estimate of the “effective” reflection site. This calculation is based on the
412 assumption that the local wave speed is constant throughout the circulation and that

413 reflection arises from a single site; both of these assumptions are questionable (48).
414 Therefore, we have refrained from estimating the location of effective reflection site(s).
415 Whether the large wave reflection contributes to persistent exercise intolerance and
416 residual symptoms post-PEA (6, 10) remains to be determined.

417 First described by Andersen and colleagues and later confirmed by Moser and Bloor,
418 it is now widely accepted that CTEPH is a dual compartment vascular disorder (3, 35)
419 with development of various degrees of secondary small-vessel arteriopathy distal to
420 both obstructed and unobstructed large arteries. Hence, despite successful
421 endarterectomy, the impact of distal vascular remodeling, which could be irreversible,
422 may be sustained and this could contribute to persistent vascular admittance
423 mismatching. Moreover, partially occluding thrombi in the distal locations may remain
424 and fragile thrombus materials may break during surgery and travel to distal vessels
425 (39) contributing to impaired pulse wave energy transmission. Post-PEA admittance
426 mismatching may also be related to post-surgery complications such as pulmonary
427 vascular steal syndrome, where previously obstructed areas become hyperperfused,
428 while non-endarterectomized areas become hypoperfused (39) or structural damage to
429 the vessel wall during surgery. Removal of tunica intima and some of the tunica media
430 of the affected vascular segments during PEA will alter the anatomy of the vessel wall
431 and cause endothelial dysfunction. (22). Regenerated endothelium has been shown to
432 exhibit impaired nitric oxide production which causes impaired vascular responses (57).
433 Further studies are warranted to determine the pathophysiology and implications of
434 persistent vascular admittance mismatching and whether it improves during longer term
435 follow-up in the same way that gas exchange capacity improves (54) and vascular steal
436 resolves (36).

437

438 **Impact of PEA on Reservoir Function**

439

440 The reservoir-excess pressure analysis offers an additional perspective on pulmonary
441 hemodynamics. Customarily, reservoir-excess pressure analysis is applied to pressures
442 acquired by high fidelity micromanometers, as fluid-filled catheters are associated with
443 issues such as damping and insufficient frequency responsiveness. However,
444 performing reservoir-excess pressure analysis on carefully acquired data using fluid-
445 filled catheters may be possible. If so, this could facilitate the use of reservoir-excess
446 pressure analysis in research and clinical settings.

447 As RV afterload increases in pulmonary hypertension, reservoir, excess and
448 asymptotic pressures increase (18, 53) and they remain high in patients with residual PH
449 following PEA. Analogous to its systemic counterpart (42), the work done by the
450 ventricle on the reservoir work represents the energy used to charge the elastic vessels
451 in systole; this provides the driving pressure for microcirculatory flow during diastole.
452 The excess pressure is the residual pressure once reservoir pressure is subtracted. Both
453 these pressures are attributable to waves. Nevertheless, excess pressure is more
454 indicative of local conditions; thus, it is noteworthy that the decrease in excess pressure
455 was related to improved RV function and reduced RV size. Reservoir pressure also
456 decreased due to the increased arterial compliance (and reduced resistance) following
457 PEA. The reduction in reservoir pressure can be viewed as an indication of improved
458 hydraulic behavior of the pulmonary circulation as the reservoir pressure represents the
459 pressure that results in the minimum ventricular hydraulic work for a given flow
460 waveform (42). This emphasizes that arterial compliance is beneficial for the system as
461 it acts as a buffer (or a “reservoir”) for pulsatile ejection.

462 The asymptotic pressure (P_{∞}) is an empirical parameter derived from the reservoir-
463 excess pressure model. It is assumed to represent the equilibrium pressure at which flow
464 out of the large elastic arteries would be expected to cease. This generally exceeds the
465 left atrial pressure due to the Starling-resistor characteristics of the lung and the
466 pulmonary microcirculatory vessels. It is assumed that near-zero pulmonary flow occurs
467 at end-diastole (21) consistent with a P_{∞} that is close to the diastolic pressure. This
468 “critical closing pressure” is influenced by vascular smooth muscle tone, pulmonary
469 rarefaction and vascular lesions as well as the alveolar pressure and gas tension (9, 30,
470 34, 43). Therefore, perhaps due to partial restoration of the pulmonary vasculature
471 following PEA, there was a marked decrease in the asymptotic pressure. It has been
472 suggested that the difference between the arterial P_{∞} and venous P_{∞} is related to
473 microcirculatory resistance (7). In support of this theory, we observed a ~41% decrease
474 in P_{∞} and the decrease was strongly correlated to the decreased PAPm and PVR.

475

476 **Diastolic Pressure Decay**

477

478 The diastolic pressure decay time is a topic of special interest in the pulmonary
479 circulation; it is usually assumed to follow a mono-exponential function determined by
480 arterial compliance and resistance. The decay time represents the time necessary for the
481 pressure to decrease to $1/e$ of the difference between P_0 (i.e. pressure at the time of
482 closure of the pulmonary valve) and the zero-flow pressure (Figure 1). For simplicity,
483 the pressure decay time is often expressed as the RC-time, calculated as the product of
484 PVR or TPR and estimated total pulmonary arterial compliance. Total pulmonary
485 arterial compliance can be derived from a Windkessel model (27); although it is
486 commonly calculated as the stroke volume to pulse pressure ratio (26, 56). It has been

487 proposed that in the pulmonary circulation, resistance and compliance are coupled
488 through an inverse hyperbolic relationship, resulting in a fixed RC-time in health and
489 disease and during treatment (4, 26, 27). A fixed RC-time implies that knowledge of
490 either resistance or compliance enables the derivation of the other parameter and that
491 RV oscillatory power remains a constant fraction of total RV power (46). However, the
492 concept of a fixed RC-time has repeatedly been challenged, as shortened RC-time has
493 been shown in CTEPH patients (31), patients with elevated PAWP (56) and subjects
494 with a PAPm < 25 mmHg (55)

495 In keeping with a previous study (31), we observed that RC_{PVR} reduced post-PEA,
496 which could be interpreted as indicating that the decrease in PVR exceeds the increase
497 in compliance. However, our observation is in direct contrast to other studies that
498 showed similar RC_{PVR} immediately following PEA (14, 50) and one year post-surgery
499 (50). We also observed that RC_{TPR} did not change significantly post-PEA, consistent
500 with another recent study (10). Finally, we observed that τ increased following PEA
501 consistent with a substantial improvement in arterial compliance. Using RC_{PVR} and
502 RC_{TPR} as estimates of pressure decay time does not take the zero-flow pressure into
503 account and assumes negligible outflow of the stroke volume during systole (47).
504 Hence, resistance-compliance products may overestimate the true pressure decay time
505 (9), especially in PH patients. Unlike RC_{PVR} and RC_{TPR} , τ does not make these
506 assumptions and therefore may be a more accurate estimate of the pressure decay time.
507 The findings of this study and previous studies (9, 19, 31, 53, 56), do not appear
508 consistent with the hypothesis of a fixed RC relationship.

509

510 **Study Limitations**

511

512 The main limitation of this study is its small size and many of the statistical
513 comparisons are probably underpowered. We pooled the data from the three pulmonary
514 artery branches together under the assumption that there is no major admittance
515 mismatch between the main, right and left pulmonary arteries as previously shown (52).
516 The absence of a difference between different branches also supports this assumption.
517 As wave power/energy is expressed per CSA of the artery, it follows that WIA is
518 potentially sensitive to vessel diameter variations. By pooling data from the three
519 pulmonary artery branches, we neglect the effect of the different diameters of main,
520 right and left PAs. PA diameter may also decrease after surgery as PAPm decreases.
521 However, a crude estimate of the main PA CSA based on cardiac output and mean flow
522 velocity showed that the change in PA area/diameter (~1 mm) was small and
523 statistically insignificant. Acquiring high quality velocity measurements was technically
524 challenging and good quality velocity data were not obtainable from the left pulmonary
525 artery from two of the patients. The pulmonary flow may be highly disturbed in PH
526 patients (25), even after PEA, causing increased signal noise and artefacts on the
527 Doppler flow tracings. Catheter whip as well as artefacts due to the vessel wall can also
528 introduce errors. Thus, careful maneuvering of the catheter during the procedure,
529 excellent quality control and meticulous data processing were necessary. Signal noises
530 and motion artefacts are particularly problematic around valve closure; however as we
531 have focused on events occurring during early and mid-systole, this was less of a
532 problem in our study.

533

534 **Conclusions**

535

WIA provides novel insights into pulmonary arterial hemodynamics. Following PEA, reservoir, excess and asymptotic pressures decreased and these changes were associated with improved RV afterload, function and size. However, despite of substantial improvements in pulmonary pressures, PVR and wave speed, a measure of pulmonary arterial stiffness, there were only small reductions in arterial wave reflection 3 months post-PEA, even in patients with a PAPm below 25 mmHg. We interpret this as indicating a lack of improvement in vascular admittance mismatch despite PEA. The possibility that this contributes to persistent exercise intolerance and residual symptoms in some patients should be explored in future.

545

546 **Glossary**

547

548 BCW: backward compression wave

549 CTEPH: chronic thromboembolic pulmonary hypertension

550 FCW: forward compression wave

551 FDW: forward decompression wave

552 PAPm: mean pulmonary arterial pressure

553 PAWP: pulmonary arterial wedge pressure

554 PEA: pulmonary endarterectomy

555 PVR: pulmonary vascular resistance

556 RC: product of resistance and compliance

557 RV: right ventricle

558 TPR, total pulmonary resistance

559 WIA: wave intensity analysis

560 WRI: wave reflection index

561 τ : diastolic time constant

562

563

564

References

1. **Abel FL.** Maximal negative dP/dt as an indicator of end of systole. *The American journal of physiology* 240: H676-679, 1981.
2. **Aguado-Sierra J, Alastruey J, Wang JJ, Hadjiloizou N, Davies J, and Parker KH.** Separation of the reservoir and wave pressure and velocity from measurements at an arbitrary location in arteries. *Proc Inst Mech Eng H* 222: 403-416, 2008.
3. **Anderson EG, Simon G, and Reid L.** Primary and thrombo-embolic pulmonary hypertension: a quantitative pathological study. *J Physiol* 110: 273-293, 1973.
4. **Bellofiore A, Wang Z, and Chesler NC.** What does the time constant of the pulmonary circulation tell us about the progression of right ventricular dysfunction in pulmonary arterial hypertension? *Pulmonary circulation* 5: 291-295, 2015.
5. **Ben-Shlomo Y, Spears M, Boustred C, May M, Anderson SG, Benjamin EJ, Boutouyrie P, Cameron J, Chen CH, Cruickshank JK, Hwang SJ, Lakatta EG, Laurent S, Maldonado J, Mitchell GF, Najjar SS, Newman AB, Ohishi M, Pannier B, Pereira T, Vasan RS, Shokawa T, Sutton-Tyrell K, Verbeke F, Wang KL, Webb DJ, Willeum HT, Zoungas S, McEniery CM, Cockcroft JR, and Wilkinson IB.** Aortic pulse wave velocity improves cardiovascular event prediction: an individual participant meta-analysis of prospective observational data from 17,635 subjects. *J Am Coll Cardiol* 63: 636-646, 2014.
6. **Bonderman D, Skoro-Sajer N, Jakowitsch J, Adlbrecht C, Dunkler D, Taghavi S, Klepetko W, Kneussl M, and Lang IM.** Predictors of outcome in chronic thromboembolic pulmonary hypertension. *Circulation* 115: 2153-2158, 2007.

- 590 7. **Bouwmeester JC, Belenkie I, Shrive NG, and Tyberg JV.** Partitioning
591 pulmonary vascular resistance using the reservoir-wave model. *J Appl Physiol (1985)*
592 115: 1838-1845, 2013.
- 593 8. **Chemla D, Castelain V, Zhu K, Papelier Y, Creuze N, Hoette S,**
594 **Parent F, Simonneau G, Humbert M, and Herve P.** Estimating right ventricular
595 stroke work and the pulsatile work fraction in pulmonary hypertension. *Chest* 143:
596 1343-1350, 2013.
- 597 9. **Chemla D, Lau EM, Papelier Y, Attal P, and Herve P.** Pulmonary
598 vascular resistance and compliance relationship in pulmonary hypertension. *The*
599 *European respiratory journal* 46: 1178-1189, 2015.
- 600 10. **Claessen G, La Gerche A, Dymarkowski S, Claus P, Delcroix M, and**
601 **Heidbuchel H.** Pulmonary vascular and right ventricular reserve in patients with
602 normalized resting hemodynamics after pulmonary endarterectomy. *Journal of the*
603 *American Heart Association* 4: e001602, 2015.
- 604 11. **Corsico AG, D'Armini AM, Cerveri I, Klersy C, Ansaldo E, Niniano**
605 **R, Gatto E, Monterosso C, Morsolini M, Nicolardi S, Tramontin C, Pozzi E, and**
606 **Vigano M.** Long-term outcome after pulmonary endarterectomy. *Am J Respir Crit Care*
607 *Med* 178: 419-424, 2008.
- 608 12. **Davies JE, Lacy P, Tillin T, Collier D, Cruickshank JK, Francis DP,**
609 **Malaweera A, Mayet J, Stanton A, Williams B, Parker KH, McG Thom SA, and**
610 **Hughes AD.** Excess pressure integral predicts cardiovascular events independent of
611 other risk factors in the conduit artery functional evaluation substudy of Anglo-
612 Scandinavian Cardiac Outcomes Trial. *Hypertension* 64: 60-68, 2014.
- 613 13. **Davies JE, Whinnett ZI, Francis DP, Willson K, Foale RA, Malik IS,**
614 **Hughes AD, Parker KH, and Mayet J.** Use of simultaneous pressure and velocity

615 measurements to estimate arterial wave speed at a single site in humans. *Am J Physiol*
616 *Heart Circ Physiol* 290: H878-H885, 2006.

617 14. **de Perrot M, McRae K, Shargall Y, Thenganatt J, Moric J, Mak S,**
618 **and Granton JT.** Early postoperative pulmonary vascular compliance predicts outcome
619 after pulmonary endarectomy for chronic thromboembolic pulmonary hypertension.
620 *Chest* 140: 34-41, 2011.

621 15. **Delcroix M, Lang I, Pepke-Zaba J, Jansa P, D'Armini AM, Snijder R,**
622 **Bresser P, Torbicki A, Mellekjaer S, Lewczuk J, Simkova I, Barbera JA, de PM,**
623 **Hoeper MM, Gaine S, Speich R, Gomez-Sanchez MA, Kovacs G, Jais X, Ambroz**
624 **D, Treacy C, Morsolini M, Jenkins D, Lindner J, Darteville P, Mayer E, and**
625 **Simonneau G.** Long-Term Outcome of Patients With Chronic Thromboembolic
626 Pulmonary Hypertension: Results From an International Prospective Registry.
627 *Circulation* 133: 859-871, 2016.

628 16. **Fedullo P, Kerr KM, Kim NH, and Auger WR.** Chronic
629 thromboembolic pulmonary hypertension. *Am J Respir Crit Care Med* 183: 1605-1613,
630 2011.

631 17. **Freed DH, Thomson BM, Berman M, Tsui SS, Dunning J, Sheares**
632 **KK, Pepke-Zaba J, and Jenkins DP.** Survival after pulmonary
633 thromboendarterectomy: effect of residual pulmonary hypertension. *J Thorac*
634 *Cardiovasc Surg* 141: 383-387, 2011.

635 18. **Ghimire A, Andersen MJ, Burrowes LM, Bouwmeester JC, Grant**
636 **AD, Belenkie I, Fine NM, Borlaug BA, and Tyberg JV.** The reservoir-wave approach
637 to characterize pulmonary vascular-right ventricular interactions in humans. *J Appl*
638 *Physiol (1985)* 121: 1348-1353, 2016.

- 639 19. **Hadinnapola C, Li Q, Su L, Pepke-Zaba J, and Toshner M.** The
640 resistance-compliance product of the pulmonary circulation varies in health and
641 pulmonary vascular disease. *Physiol Rep* 3: 2015.
- 642 20. **Hametner B, Wassertheurer S, Hughes AD, Parker KH, Weber T,**
643 **and Eber B.** Reservoir and excess pressures predict cardiovascular events in high-risk
644 patients. *Int J Cardiol* 171: 31-36, 2014.
- 645 21. **Harvey RM, Enson Y, and Ferrer MI.** A reconsideration of the origins
646 of pulmonary hypertension. *Chest* 59: 82-94, 1971.
- 647 22. **Jenkins D.** Pulmonary endarterectomy: the potentially curative treatment
648 for patients with chronic thromboembolic pulmonary hypertension. *Eur Respir Rev* 24:
649 263-271, 2015.
- 650 23. **Jones CJ, and Sugawara M.** "Wavefronts" in the aorta--implications for
651 the mechanisms of left ventricular ejection and aortic valve closure. *Cardiovasc Res* 27:
652 1902-1905, 1993.
- 653 24. **Khiri AW, O'Brien A, Gibbs JS, and Parker KH.** Determination of
654 wave speed and wave separation in the arteries. *J Biomech* 34: 1145-1155, 2001.
- 655 25. **Kondo C, Caputo GR, Masui T, Foster E, O'Sullivan M, Stulbarg MS,**
656 **Golden J, Catterjee K, and Higgins CB.** Pulmonary hypertension: pulmonary flow
657 quantification and flow profile analysis with velocity-encoded cine MR imaging.
658 *Radiology* 183: 751-758, 1992.
- 659 26. **Lankhaar JW, Westerhof N, Faes TJ, Gan CT, Marques KM,**
660 **Boonstra A, van den Berg FG, Postmus PE, and Vonk-Noordegraaf A.** Pulmonary
661 vascular resistance and compliance stay inversely related during treatment of pulmonary
662 hypertension. *Eur Heart J* 29: 1688-1695, 2008.

- 663 27. **Lankhaar JW, Westerhof N, Faes TJ, Marques KM, Marcus JT,**
664 **Postmus PE, and Vonk-Noordegraaf A.** Quantification of right ventricular afterload
665 in patients with and without pulmonary hypertension. *Am J Physiol Heart Circ Physiol*
666 291: H1731-H1737, 2006.
- 667 28. **Lau EM, Abelson D, Dwyer N, Yu Y, Ng MK, and Celermajer DS.**
668 Assessment of ventriculo-arterial interaction in pulmonary arterial hypertension using
669 wave intensity analysis. *Eur Respir J* 43: 1804-1807, 2014.
- 670 29. **Laurent S, Boutouyrie P, Asmar R, Gautier I, Laloux B, Guize L,**
671 **Ducimetiere P, and Benetos A.** Aortic stiffness is an independent predictor of all-cause
672 and cardiovascular mortality in hypertensive patients. *Hypertension* 37: 1236-1241,
673 2001.
- 674 30. **Lopez-Muniz R, Stephens NL, Bromberger-Barnea B, Permutt S, and**
675 **Riley RL.** Critical closure of pulmonary vessels analyzed in terms of Starling resistor
676 model. *Journal of applied physiology* 24: 625-635, 1968.
- 677 31. **MacKenzie Ross RV, Toshner MR, Soon E, Naeije R, and Pepke-Zaba**
678 **J.** Decreased time constant of the pulmonary circulation in chronic thromboembolic
679 pulmonary hypertension. *Am J Physiol Heart Circ Physiol* 305: H259-H264, 2013.
- 680 32. **Mahapatra S, Nishimura RA, Oh JK, and McGoon MD.** The
681 prognostic value of pulmonary vascular capacitance determined by Doppler
682 echocardiography in patients with pulmonary arterial hypertension. *J Am Soc*
683 *Echocardiogr* 19: 1045-1050, 2006.
- 684 33. **Mahapatra S, Nishimura RA, Sorajja P, Cha S, and McGoon MD.**
685 Relationship of pulmonary arterial capacitance and mortality in idiopathic pulmonary
686 arterial hypertension. *J Am Coll Cardiol* 47: 799-803, 2006.

- 687 34. **Mayers I, and Johnson DH.** Vasodilators do not abolish pulmonary
688 vascular critical closing pressure. *Respiration physiology* 81: 63-73, 1990.
- 689 35. **Moser KM, and Bloor CM.** Pulmonary vascular lesions occurring in
690 patients with chronic major vessel thromboembolic pulmonary hypertension. *Chest* 103:
691 685-692, 1993.
- 692 36. **Moser KM, Metersky ML, Auger WR, and Fedullo PF.** Resolution of
693 vascular steal after pulmonary thromboendarterectomy. *Chest* 104: 1441-1444, 1993.
- 694 37. **Mynard JP, Penny DJ, Davidson MR, and Smolich JJ.** The reservoir-
695 wave paradigm introduces error into arterial wave analysis: a computer modelling and
696 in-vivo study. *J Hypertens* 30: 734-743, 2012.
- 697 38. **Narayan O, Davies JE, Hughes AD, Dart AM, Parker KH, Reid C,**
698 **and Cameron JD.** Central aortic reservoir-wave analysis improves prediction of
699 cardiovascular events in elderly hypertensives. *Hypertension* 65: 629-635, 2015.
- 700 39. **Olman MA, Auger WR, Fedullo PF, and Moser KM.** Pulmonary
701 vascular steal in chronic thromboembolic pulmonary hypertension. *Chest* 98: 1430-
702 1434, 1990.
- 703 40. **Parker KH.** Arterial reservoir pressure, subservient to the McDonald
704 lecture, Artery 13. *Artery Research* 7: 171-185, 2013.
- 705 41. **Parker KH.** An introduction to wave intensity analysis. *Med Biol Eng*
706 *Comput* 47: 175-188, 2009.
- 707 42. **Parker KH, Alastruey J, and Stan GB.** Arterial reservoir-excess
708 pressure and ventricular work. *Med Biol Eng Comput* 50: 419-424, 2012.
- 709 43. **Permutt S, and Riley RL.** Hemodynamics of collapsible vessels with
710 tone: the vascular waterfall. *J Appl Physiol* 18: 924-932, 1963.

- 711 44. **Quail MA, Knight DS, Steeden JA, Taelman L, Moledina S, Taylor**
712 **AM, Segers P, Coghlan GJ, and Muthurangu V.** Noninvasive pulmonary artery wave
713 intensity analysis in pulmonary hypertension. *Am J Physiol Heart Circ Physiol* 308:
714 H1603-H1611, 2015.
- 715 45. **Reynolds DW, Bartelt N, Taepke R, and Bennett TD.** Measurement of
716 pulmonary artery diastolic pressure from the right ventricle. *Journal of the American*
717 *College of Cardiology* 25: 1176-1182, 1995.
- 718 46. **Saouti N, Westerhof N, Helderma F, Marcus JT, Boonstra A,**
719 **Postmus PE, and Vonk-Noordegraaf A.** Right ventricular oscillatory power is a
720 constant fraction of total power irrespective of pulmonary artery pressure. *Am J Respir*
721 *Crit Care Med* 182: 1315-1320, 2010.
- 722 47. **Segers P, Brimiouille S, Stergiopulos N, Westerhof N, Naeije R,**
723 **Maggiorini M, and Verdonck P.** Pulmonary arterial compliance in dogs and pigs: the
724 three-element windkessel model revisited. *Am J Physiol* 277: H725-H731, 1999.
- 725 48. **Segers P, O'Rourke MF, Parker K, Westerhof N, and Hughes A.**
726 Towards a consensus on the understanding and analysis of the pulse waveform: Results
727 from the 2016 Workshop on Arterial Hemodynamics: Past, present and future. *Artery*
728 *Res* 18: 75-80, 2017.
- 729 49. **Segers P, Swillens A, and Vermeersch S.** Reservations on the reservoir.
730 *J Hypertens* 30: 676-678, 2012.
- 731 50. **Skoro-Sajer N, Marta G, Gerges C, Hlavin G, Nierlich P, Taghavi S,**
732 **Sadushi-Kolici R, Klepetko W, and Lang IM.** Surgical specimens, haemodynamics
733 and long-term outcomes after pulmonary endarterectomy. *Thorax* 69: 116-122, 2014.

- 734 51. **Su J, Hilberg O, Howard L, Simonsen U, and Hughes AD.** A review of
 735 wave mechanics in the pulmonary artery with an emphasis on wave intensity analysis.
 736 *Acta Physiol (Oxf)* 218: 239-249, 2016.
- 737 52. **Su J, Manisty C, Parker KH, Simonsen U, Nielsen-Kudsk JE,**
 738 **Mellemkjaer S, Connolly S, Lim PB, Whinnett ZI, Malik IS, Watson G, Davies JE,**
 739 **Gibbs S, Hughes AD, and Howard LS.** Wave Intensity Analysis Provides Novel
 740 Insights into Pulmonary Arterial Hypertension and Chronic Thromboembolic
 741 Pulmonary Hypertension. *J Am Heart Assoc* 6: e006679, 2017.
- 742 53. **Su J, Manisty C, Simonsen U, Howard LS, Parker KH, and Hughes**
 743 **AD.** Pulmonary artery wave propagation and reservoir function in conscious man:
 744 impact of pulmonary vascular disease, respiration and dynamic stress tests. *J Physiol*
 745 595: 6463-6476, 2017.
- 746 54. **Tanabe N, Okada O, Nakagawa Y, Masuda M, Kato K, Nakajima N,**
 747 **and Kuriyama T.** The efficacy of pulmonary thromboendarterectomy on long-term gas
 748 exchange. *Eur Respir J* 10: 2066-2072, 1997.
- 749 55. **Tedford RJ.** Determinants of right ventricular afterload (2013 Grover
 750 Conference series). *Pulmonary circulation* 4: 211-219, 2014.
- 751 56. **Tedford RJ, Hassoun PM, Mathai SC, Girgis RE, Russell SD,**
 752 **Thiemann DR, Cingolani OH, Mudd JO, Borlaug BA, Redfield MM, Lederer DJ,**
 753 **and Kass DA.** Pulmonary capillary wedge pressure augments right ventricular pulsatile
 754 loading. *Circulation* 125: 289-297, 2012.
- 755 57. **Vanhoutte PM.** Regeneration of the endothelium in vascular injury.
 756 *Cardiovasc Drugs Ther* 24: 299-303, 2010.
- 757 58. **Vermeersch SJ, Rietzschel ER, De Buyzere ML, Van Bortel LM,**
 758 **Gillebert TC, Verdonck PR, and Segers P.** The reservoir concept: the 3-element

759 windkessel model revisited? Application to the Asklepios population study. *J Eng Math*
760 64: 417-428, 2009.

761 59. **Wang JJ, O'Brien AB, Shrive NG, Parker KH, and Tyberg JV.** Time-
762 domain representation of ventricular-arterial coupling as a windkessel and wave system.
763 *Am J Physiol Heart Circ Physiol* 284: H1358-H1368, 2003.

764 60. **Womersley JR.** Oscillatory flow in arteries. II. The reflection of the pulse
765 wave at junctions and rigid inserts in the arterial system. *Phys Med Biol* 2: 313-323,
766 1958.

767

768

769 **Additional information**

770

771 **Competing interests**

772 None.

773

774 **Author contributions**

775

776 The study was carried out at Hammersmith Hospital, Imperial College Healthcare
777 NHS Trust, London and Aarhus University Hospital. J.S., A.D.H., U.S. and K.H.P.
778 conceived and designed the experiment. J.S., J.E.N.K, L.S.H and S.M. collected the
779 experimental data. J.S., A.D.H., K.H.P., L.S.H. and S.M. performed data analysis and
780 interpretation. J.S. drafted the paper and all authors revised it critically for important
781 intellectual content. All authors have approved the final version of the manuscript and
782 agree to be accountable for all aspects of the work. All persons designated as authors
783 qualify for authorship, and all those who qualify for authorship are listed.

784

785 **Funding**

786

787 J.S. received support from the European Respiratory Society ERS PAH Long-Term
788 Research fellowship (n° LTRF 2013-2183) and Aarhus University Graduate School.
789 A.D.H..received support from the British Heart Foundation (CS/13/1/30327,
790 PG/13/6/29934, PG/15/75/31748, CS/15/6/31468, PG/17/90/33415, IG/18/5/33958), the
791 National Institute for Health Research University College London Hospitals Biomedical
792 Research Centre, the UK Medical Research Council (MR/P023444/1) and works in a
793 unit that receives support from the UK Medical Research Council (MC_UU_12019/1).

794 L.S.H. received support from a National Institute for Health Research Biomedical
795 Research Centre Award to Imperial Healthcare NHS Trust. The funders played no role
796 in preparation of the manuscript or decision to publish.

797

798 **Figure 1: Schematic of the Diastolic Pressure Decay**

799 P_0 is the pressure at time, t_0 , corresponding to the end of ventricular ejection (pulmonary
800 valve closes). This was assumed to correspond to the time of maximal negative dP/dt .
801 The asymptotic pressure (P_∞) is the limit for the exponential decay of the pressure
802 during diastole and corresponds to the pressure at which outflow through the
803 microcirculation would be predicted to be zero assuming a mono-exponential decay.
804 The pressure decay time, i.e. the time constant, τ , represents the time necessary for the
805 pressure to decrease to $1/e$ of the difference between P_0 and P_∞ .

806

807 **Figure 2: Wave Intensity Analysis**

808 Measured pressure and flow velocity profile in the main pulmonary artery and the
809 corresponding wave intensity (WI) patterns are shown for a patient (**A, B**) before and
810 (**C, D**) after pulmonary endarterectomy (PEA). For comparison, (**E, F**) a WI pattern
811 from a representative control subject without pulmonary vascular disease from a
812 previous study (52) is also shown. The contour of the net wave intensity is highlighted
813 in red. Following PEA, pulmonary arterial pressure decreased (mean pulmonary artery
814 pressure < 25 mmHg) and velocity increased (signal noises and motion artefacts can be
815 seen in end-systole). The three dominant systolic waves observed are: forward
816 compression wave (FCW) related to right ventricular contraction, forward
817 decompression wave (FDW) related to ventricular relaxation and backward
818 compression wave (BCW) due to wave reflection. Note that large BCW persisted after
819 surgery. In contrast, the control subject displayed a negligible BCW.

820

821 **Figure 3: Post-Surgery Wave Intensity Parameters**

Wave intensity parameters, specifically (A) wave speed, (B) forward compression wave (FCW) energy and (C) wave reflection index (WRI) of the patients after pulmonary endarterectomy (PEA) and of control subjects without pulmonary vascular disease (N = 10) from a previous study (52) are presented here. Post-PEA patients are separated into two groups: those with a mean pulmonary arterial pressure (PAPm) < 25 mmHg (N = 3) and those with residual pulmonary hypertension (res. PH, N = 5). Note that patients with PAPm < 25 mmHg remained to have substantially larger wave reflection compared to controls. Data are presented as estimated marginal means (pooled data from the main and branch pulmonary arteries) and SE and analyzed using mixed linear models.

831

832 **Figure 4: Reservoir-excess Pressure Analysis**

833 Separation of the measured pressure from the main pulmonary artery into a reservoir pressure and an excess pressure and superimposition of the excess pressure waveform on to the velocity waveform (scaled so that the peaks of the waveforms coincide) are shown for a patient (A, B) before and (C, D) after pulmonary endarterectomy (PEA). For comparison, (E, F) reservoir and excess pressure profiles for a representative control subject without pulmonary vascular disease from a previous study (52) is also shown. Both the reservoir and excess pressures decreased following surgery (note the scale difference). The morphology of the flow velocity waveform deviated from the excess pressure waveform in mid-systole, where there is a rapid initial decrease in the velocity before the velocity plateaus. This is not matched in the excess pressure waveform consistent with wave reflection. In contrast, the flow velocity waveform resembled the excess pressure waveform of the control subject consistent with minimal wave reflection. (Same patients as in figure 1).

846

847 **Figure 5: Post-Surgery Reservoir Indices**

848 Indices derived from reservoir-excess pressure analysis, specifically the (A) peak
849 reservoir pressure, (B) peak excess pressure and (C) asymptotic pressure of the patients
850 after pulmonary endarterectomy (PEA) and of control subjects without pulmonary
851 vascular disease (N = 10) from a previous study (52) are presented here. Post-PEA
852 patients are separated into two groups: those with a mean pulmonary arterial pressure
853 (PAPm) < 25 mmHg (N = 3) and those with residual pulmonary hypertension (res. PH,
854 N = 5). Data are presented as estimated marginal means (pooled data from the main and
855 branch pulmonary arteries) and SE and analyzed using mixed linear models.

856

857 **Figure 6: Relationship Between the Estimated Diastolic Time Constants τ , RC_{PVR}**
858 **and RC_{TPR}**

859 τ is the inverse of the diastolic rate constant, RC_{TPR} is product of total pulmonary
860 vascular resistance and compliance and RC_{PVR} is the product of pulmonary vascular
861 resistance and compliance. PEA: pulmonary endarterectomy

862

863

864

865

866

867 **Table 1.** Patient Symptoms and Hemodynamic Measurements

868

N = 8	†Pre-PEA	Post-PEA	Δ
WHO function class, I/ II/ III/ IV, N	0/ 1/ 7/ 0	3/ 3/ 2/ 0	--
Heart rate, min ⁻¹	83 ± 14	80 ± 11	-3 [-16; 10]
Systolic BP, mmHg	129 ± 22	134 ± 17	5 [-11; 21]
Diastolic BP, mmHg	87 ± 19	86 ± 9	-6 [-15; 12]
Cardiac output, l/min	4.1 ± 1.8	5.4 ± 2.2	1.3 [0.4; 2.2]*
Right atrial pressure, mmHg	12 ± 5	8 ± 5	-5 [-11; 1]
Systolic PAP, mmHg	82 ± 14	55 ± 22	-27 [-47; -7]*
Diastolic PAP, mmHg	32 ± 9	21 ± 9	-11 [-23; 1]
Mean PAP, mmHg	49 ± 10	32 ± 13	-16 [-31; -2]*
PAWP, mmHg	9 ± 3	10 ± 3	1 [-3; 4]
PVR, Wood Units	11.1 ± 4.3	5.1 ± 4.4	-6.1 [-10.5; -1.6]*
Peak velocity in main PA, cm/s	38.7 ± 12.0	55.7 ± 22.4	17.1 [3.1; 30.9]*
Mean velocity in main PA, cm/s	21.0 ± 7.1	31.6 ± 11.9	10.6 [3.1; 18.1]*
Arterial compliance, ml/mmHg	1.0 ± 0.3	2.2 ± 0.9	1.2 [0.5; 2.0]*
RV stroke work, ml·mmHg	1895 ± 987	1714 ± 1291	-181 [-1246; 883]

869

870 Abbreviations: BP, blood pressure; PAP, pulmonary arterial pressure; PA: pulmonary

871 artery, PAWP, pulmonary artery wedge pressure; PEA, pulmonary endarterectomy;

872 PVR, pulmonary vascular resistance; RV, right ventricle; WHO, World Health

873 Organization

874 Data are presented as mean ± SD and the differences between pre- and post-PEA data

875 (post – pre) are presented with 95 % CI.

876 *p < 0.05 versus pre-PEA.

877 †Pre-PEA data from 6 of these patients have been included in a previous study (52).

878 **Table 2.** Wave Characteristics

	Pre-PEA	Post-PEA	Δ
Wave speed	16.5 [14.8; 18.2]	8.10 [6.33; 9.87]	-8.39 [-10.85; -5.93]*
Ln (FCW intensity, kW/m ²)	11.7 [11.4; 12.0]	11.7 [11.4; 11.9]	-0.04 [-0.31; 0.24]
Ln (FCW energy, kJ/m ²)	8.64 [8.40; 8.88]	8.67 [8.43; 8.91]	0.03 [-0.14; 0.21]
Ln (BCW intensity, kW/m ²)	10.4 [10.1; 10.7]	10.0 [9.7; 10.3]	-0.42 [-0.84; -0.01]*
Ln (BCW energy, kJ/m ²)	7.24 [6.93; 7.56]	6.93 [6.61; 7.26]	-0.31 [-0.72; 0.10]
Wave reflection index, %	27.6 [22.8; 32.4]	21.5 [16.5; 26.4]	-6.15 [-13.0; 0.7]
Ln (FCW to RV power density ratio)	4.89 [4.64; 5.14]	4.94 [4.68; 5.19]	0.05 [-0.31; 0.40]
Ln (FCW to RV energy density ratio)	5.19 [4.96; 5.42]	5.20 [4.96; 5.43]	0.01 [-0.32; 0.34]

879

880 Abbreviations: BCW, backward compression wave; FCW, forward compression wave;

881 PEA, pulmonary endarterectomy.

882 Data from the main, right and left pulmonary arteries were pooled together and

883 presented as estimated marginal means [95 % CI] derived from a mixed linear model.

884 Note that FCW intensity and energy exceeds RV power and energy (ratio > 1). This is

885 because wave intensity and energy were normalized to the length of the cardiac cycle

886 (Equation 5).

887 *p < 0.05 versus pre-PEA.

888 †Pre-PEA data from 6 of these patients have been included in a previous study (52).

889

890

891 **Table 3.** Reservoir Function

N = 8	Pre-PEA	Post-PEA	Δ
Reservoir-excess pressure analysis			
Asymptotic pressure, mmHg	31.5 [26.3; 36.8]	21.1 [15.8; 26.3]	-10.5 [-15.4; -5.6]*
Peak reservoir pressure, mmHg	32.6 [28.1; 37.2]	20.9 [16.4; 25.5]	-11.7 [-14.8; -8.6]*
Reservoir pressure integral, mmHg·s	9.85 [8.52; 11.19]	6.53 [5.19; 7.86]	-3.33 [-4.20; -2.45]*
Peak excess pressure, mmHg	23.0 [19.6; 26.5]	17.8 [14.3; 21.3]	-5.21 [-7.23; -3.20]*
Excess pressure integral, mmHg·s	4.78 [4.07; 5.49]	3.65 [2.94; 4.36]	-1.13 [-1.61; -0.65]*
Ln (Systolic rate constant, s ⁻¹)	2.64 [2.43; 2.85]	2.39 [2.18; 2.60]	-0.25 [-0.44; -0.07]*
Diastolic rate constant, s ⁻¹	7.17 [5.58; 8.75]	5.07 [3.48; 6.65]	-2.10 [-3.11; -1.09]*
Diastolic pressure decay time			
τ , s	0.17 [0.13; 0.22]	0.23 [0.19; 0.28]	0.06 [0.02; 0.10]*
RC _{PVR} , s	0.60 ± 0.15	0.49 ± 0.13	0.11 [0.00; 0.22]
RC _{TPR} , s	0.75 ± 0.21	0.75 ± 0.18	0.00 [-0.16; 0.16]

892
893

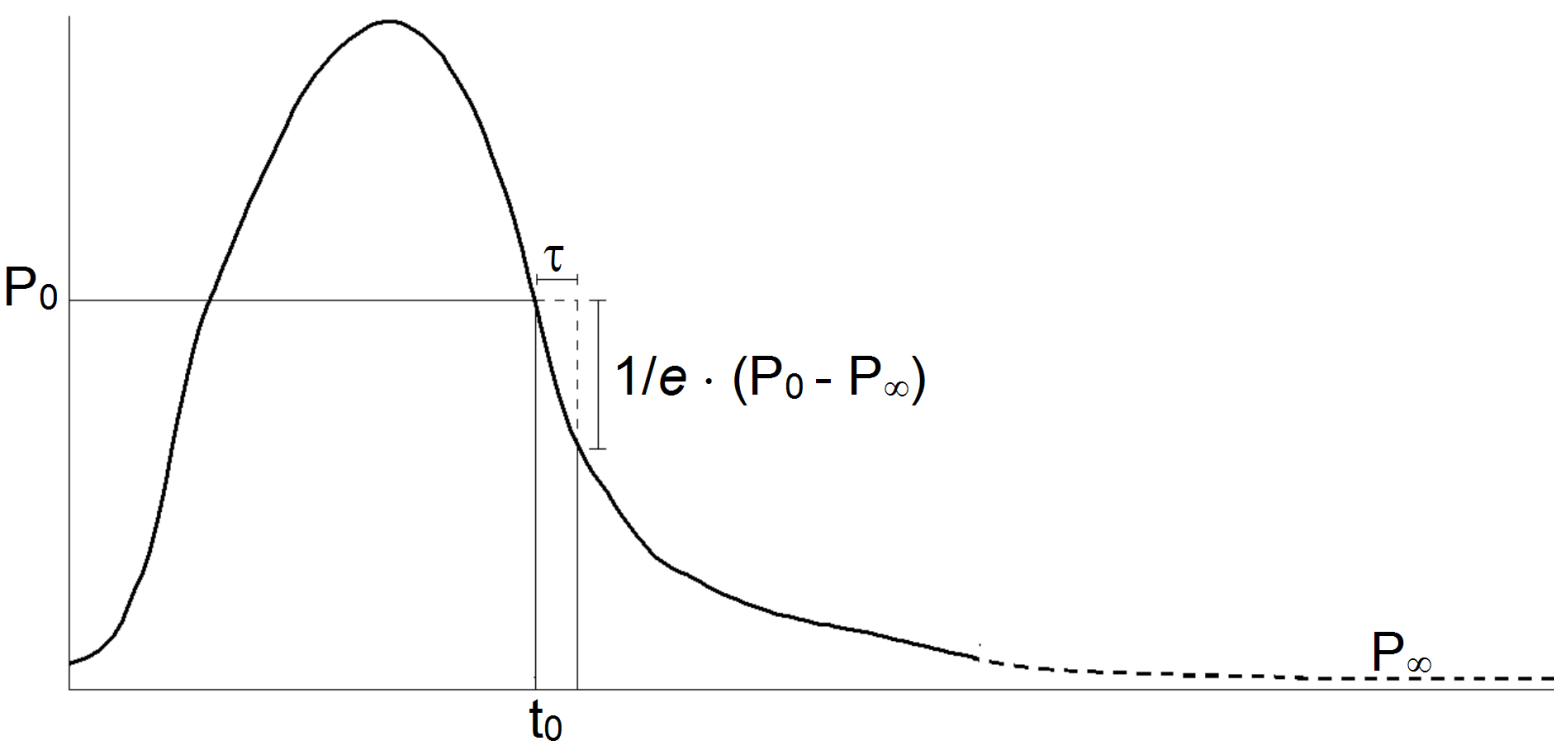
894 Abbreviations: PEA, pulmonary endarterectomy; RC_{PVR}, product of pulmonary vascular
895 resistance and compliance; RC_{TPR}, product of total pulmonary resistance and
896 compliance; τ , diastolic time constant.

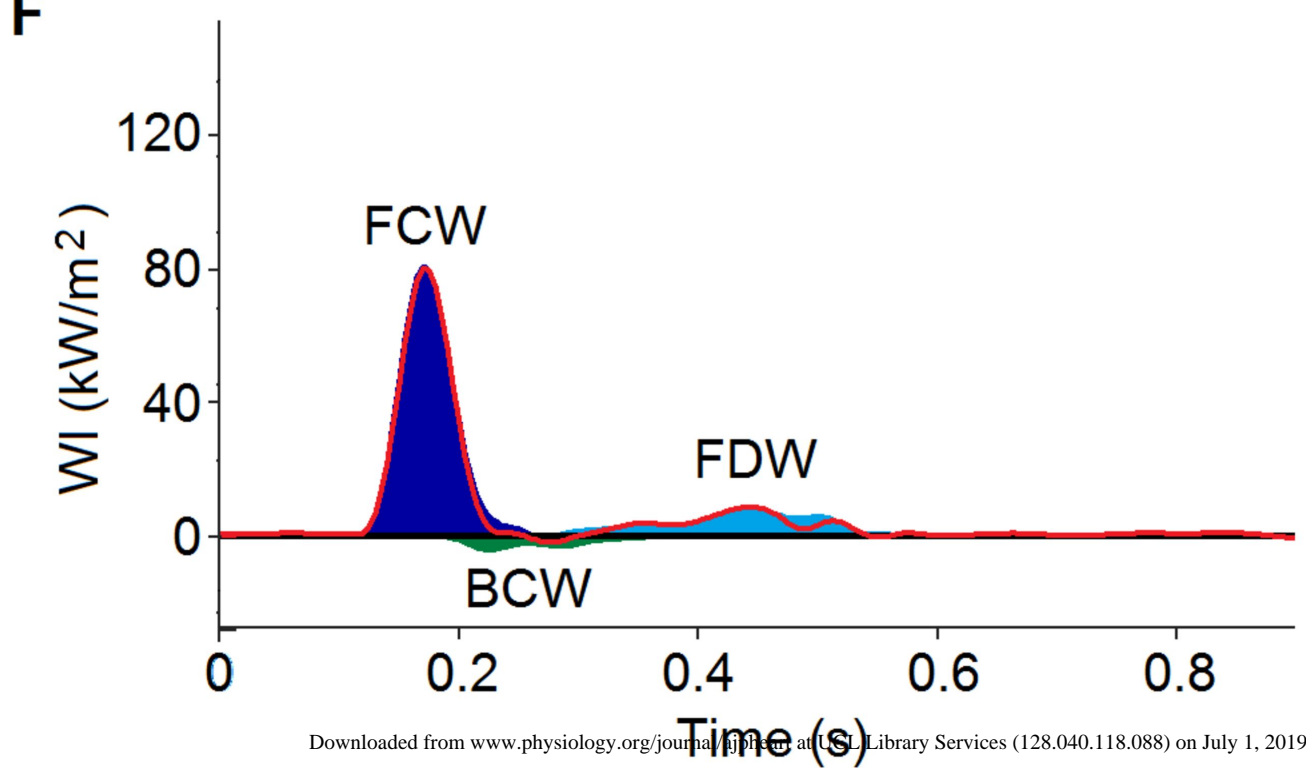
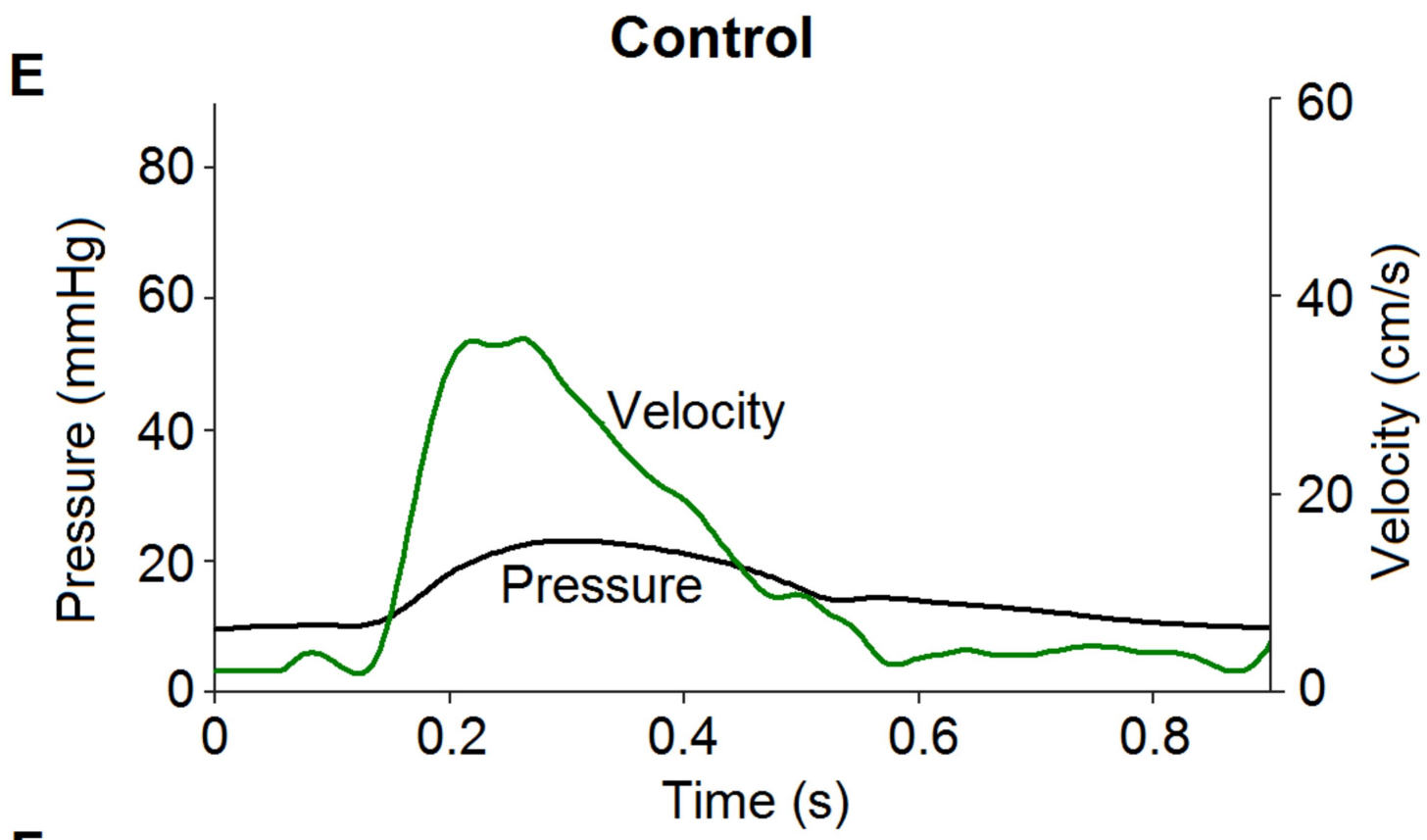
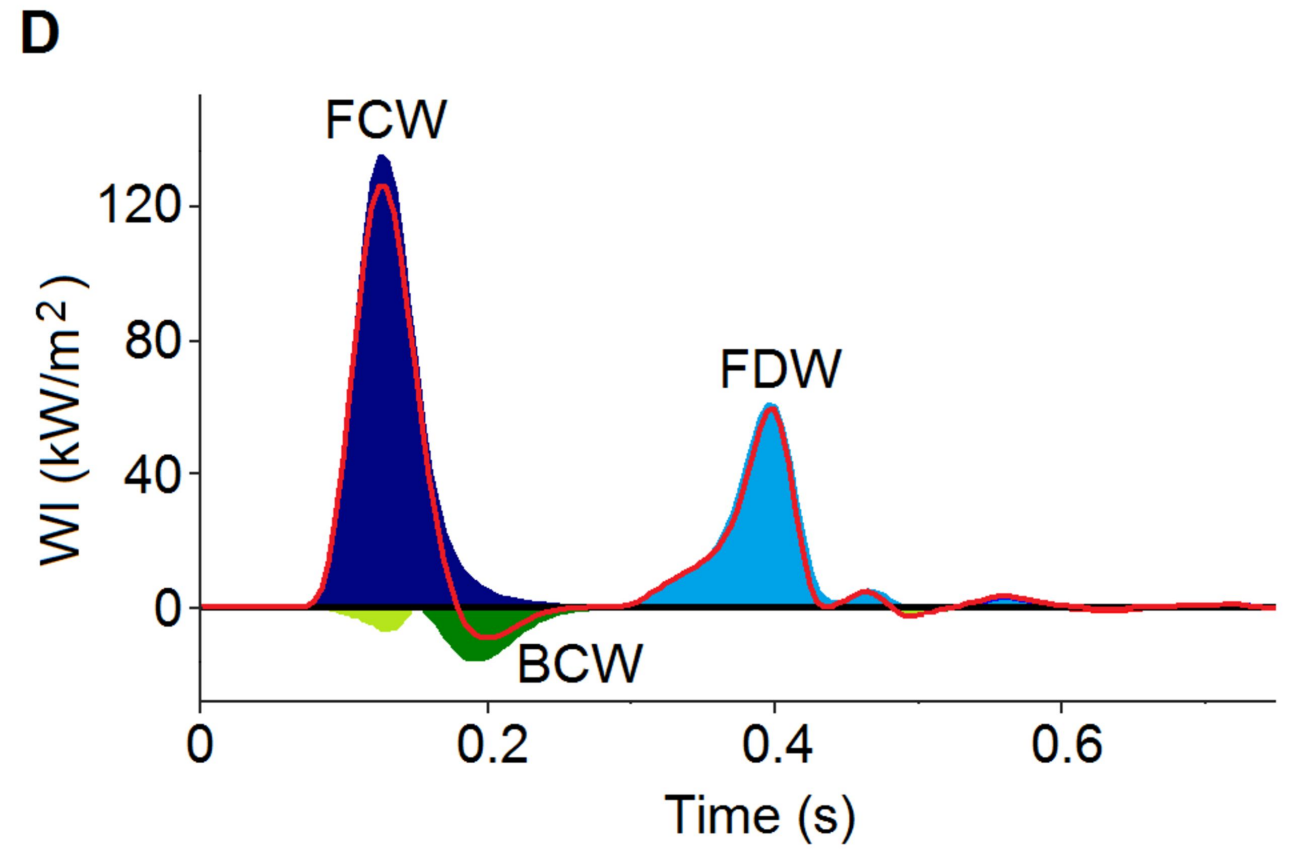
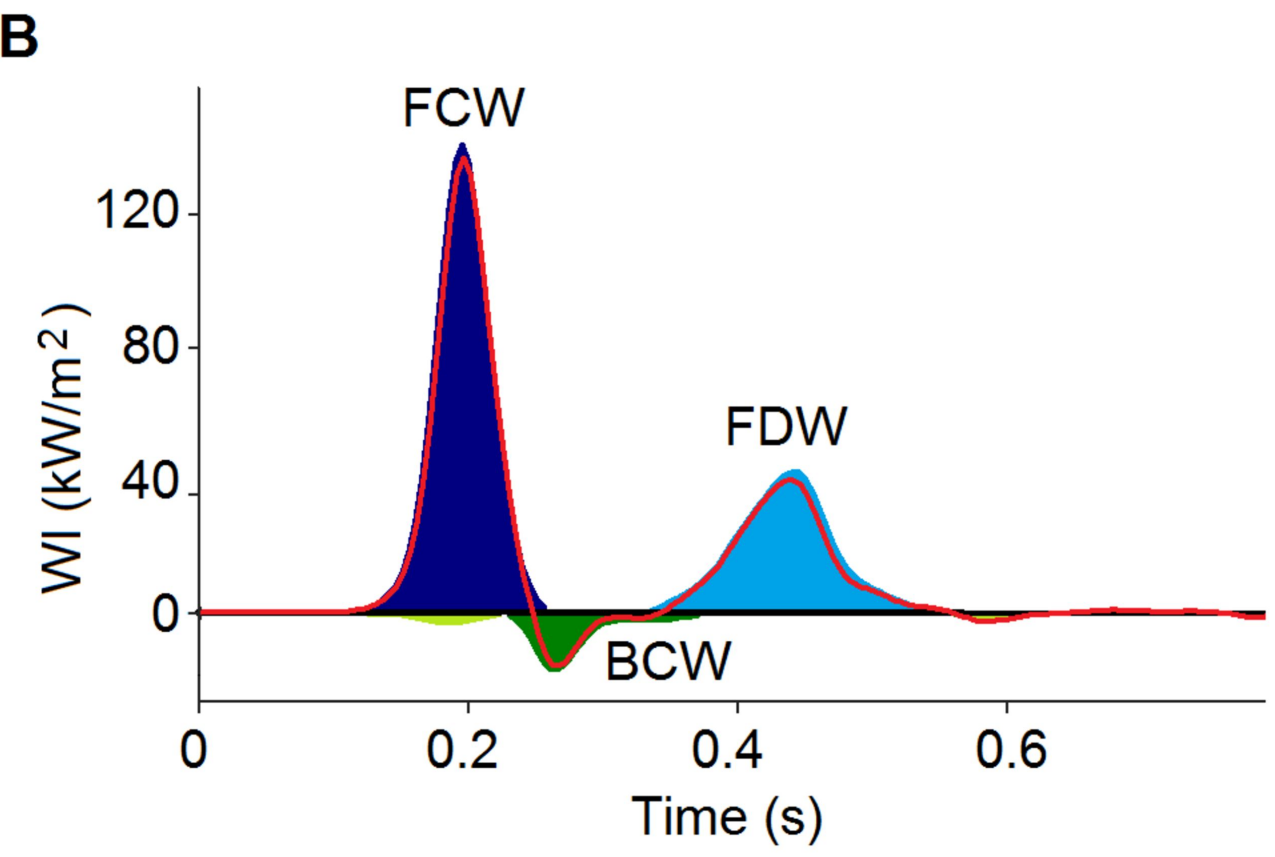
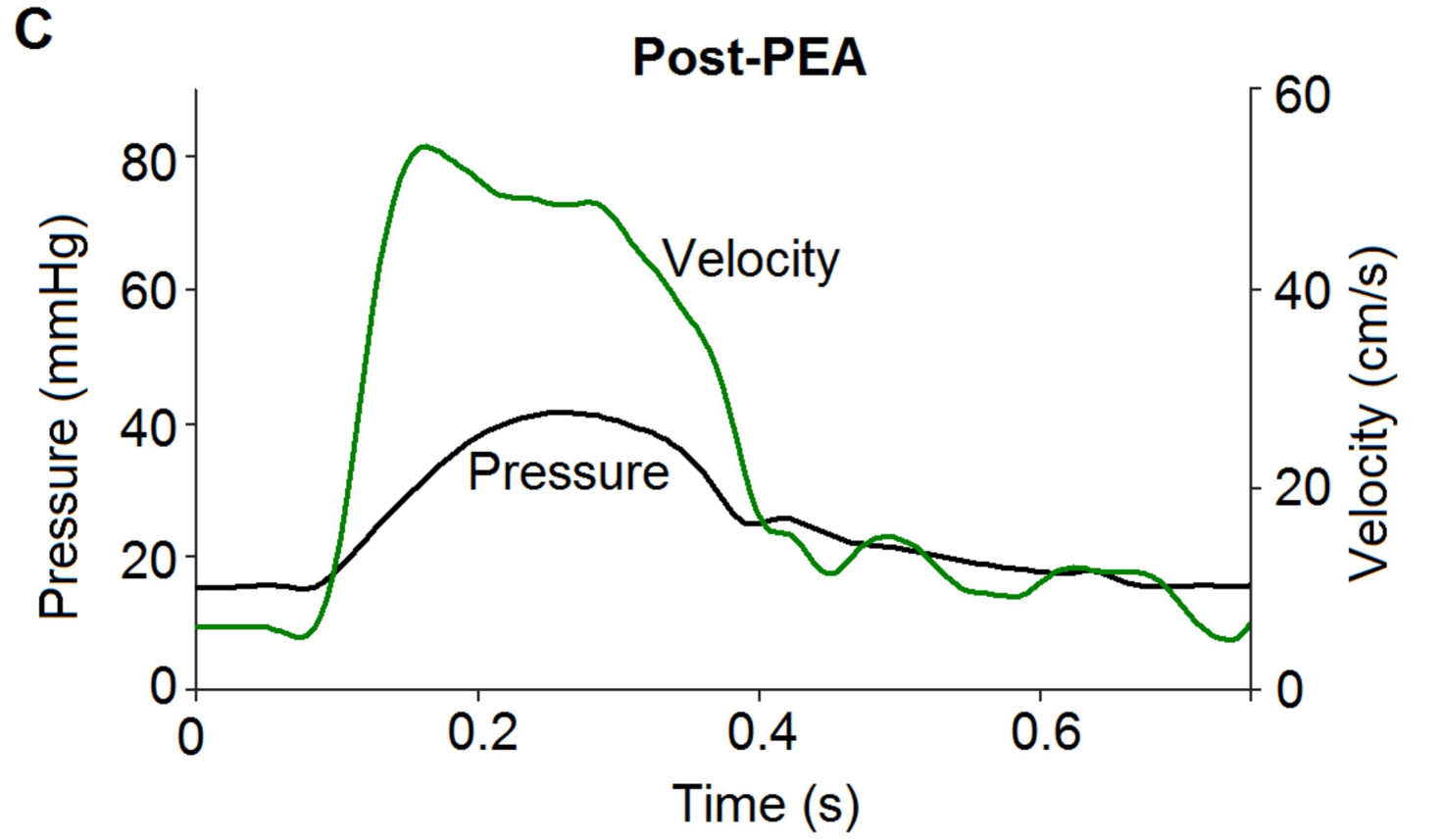
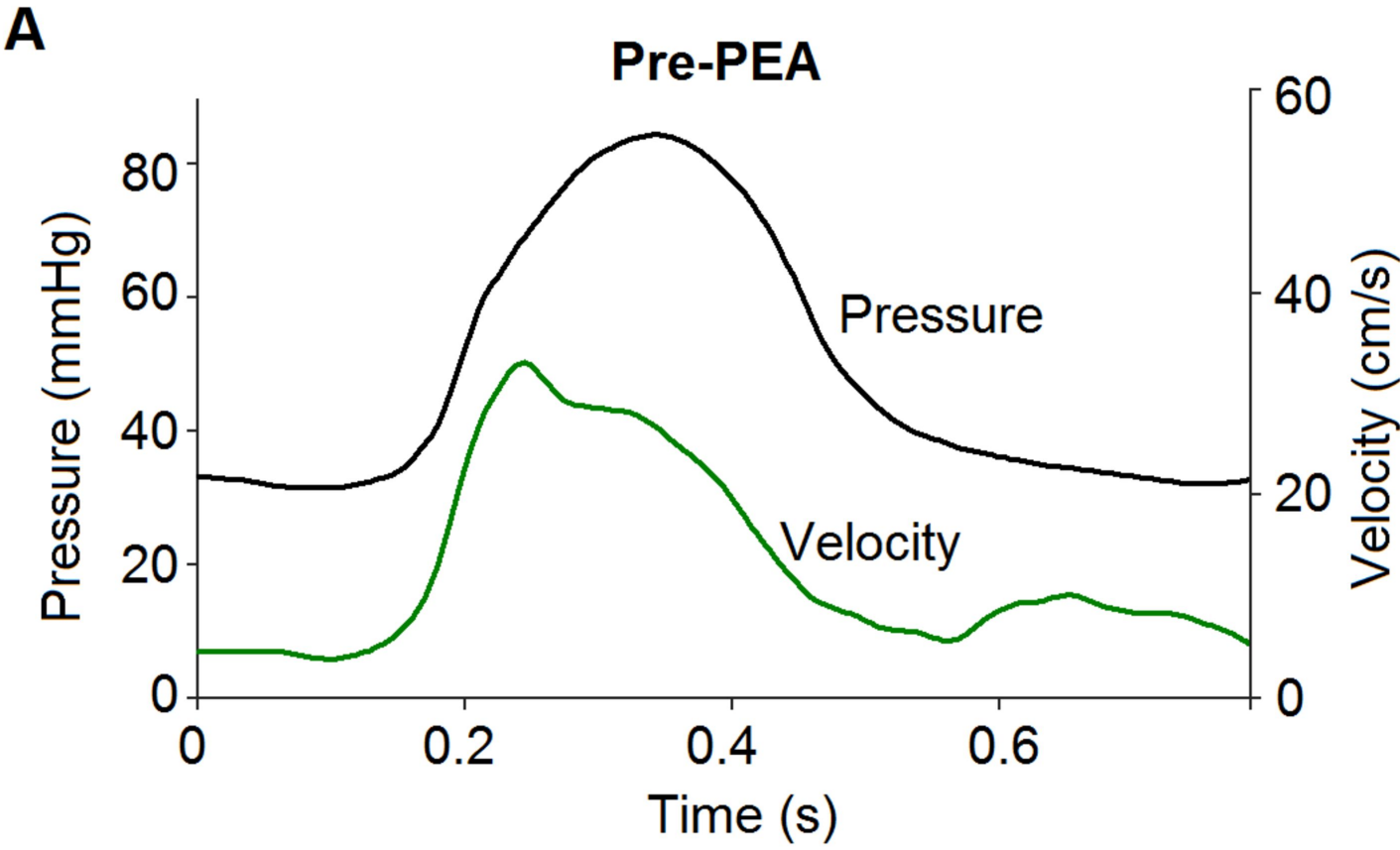
897 Data from the main, right and left pulmonary arteries were pooled together and
898 presented as estimated marginal means [95 % CI] derived from a mixed linear model.

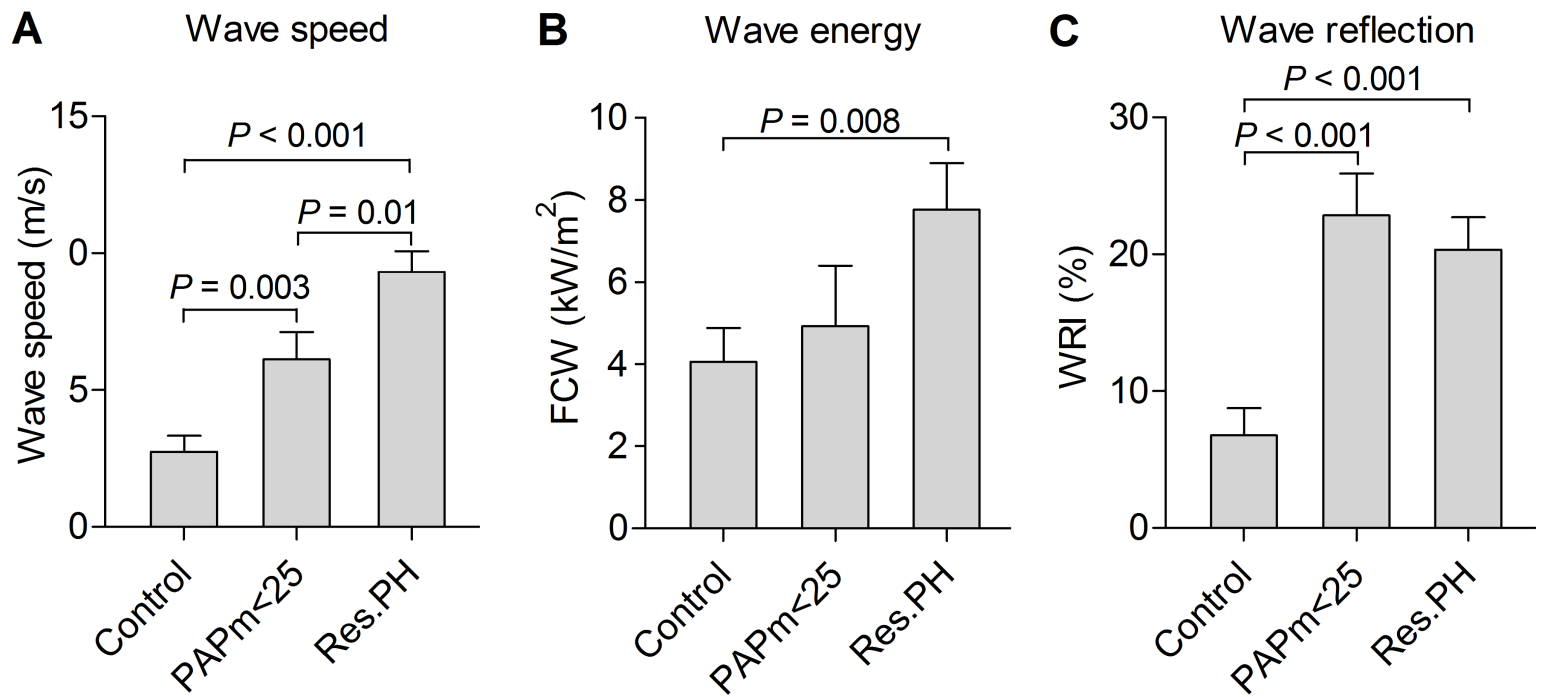
899 RC_{PVR} and RC_{TPR} are presented as mean ± SD.

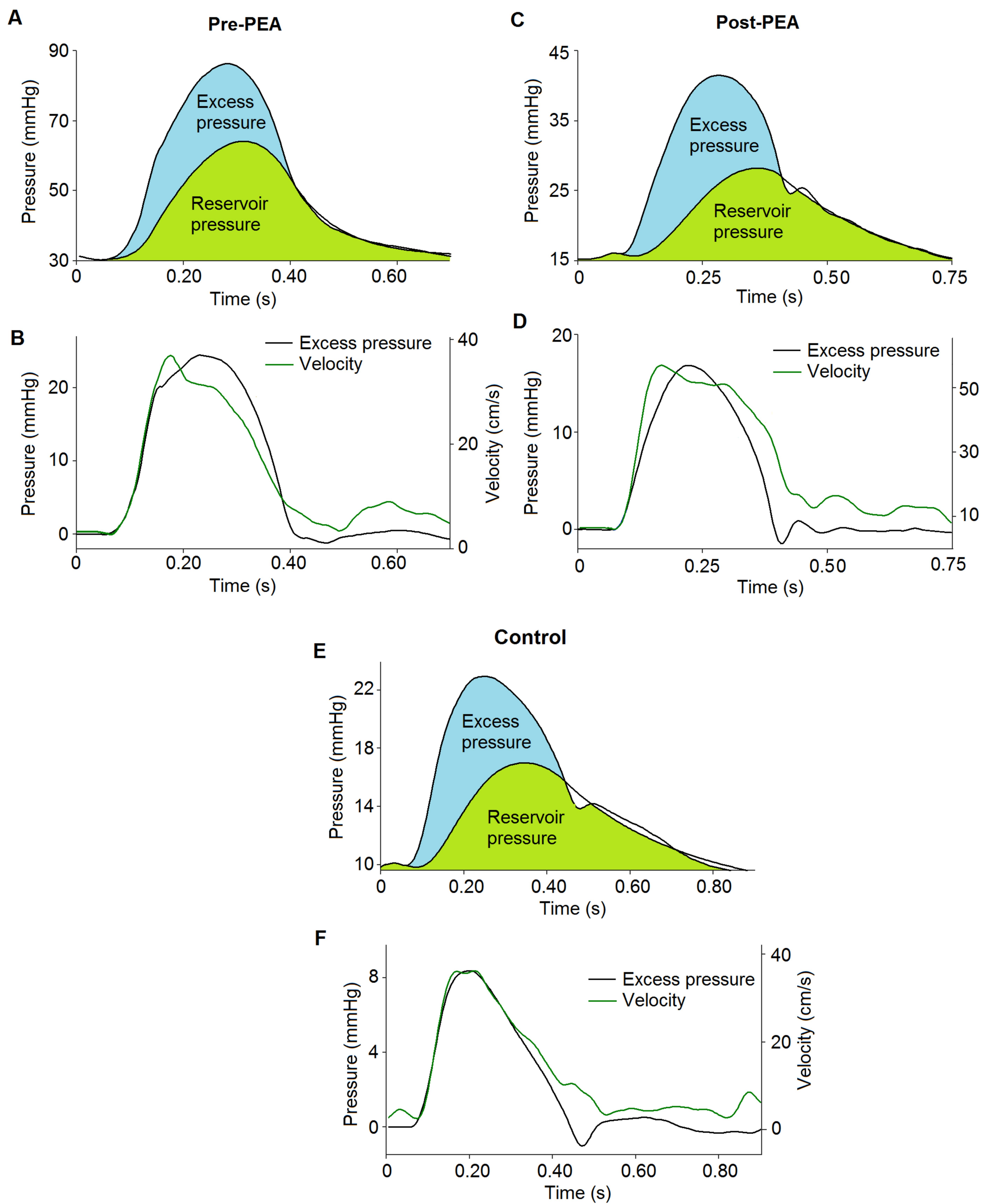
900 *p < 0.05 versus pre-PEA.

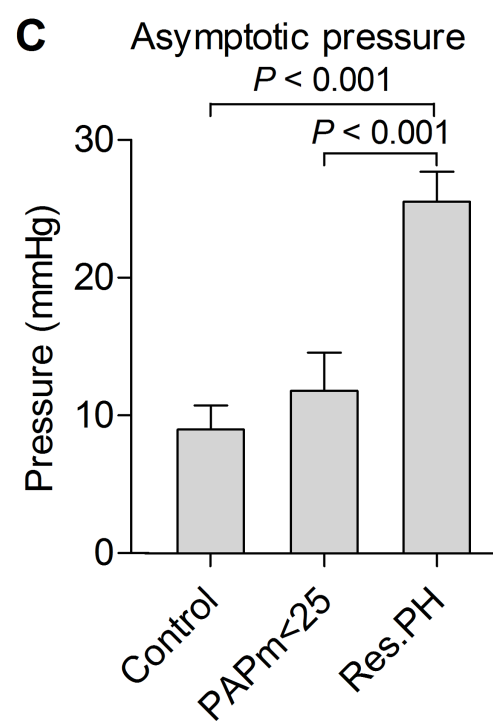
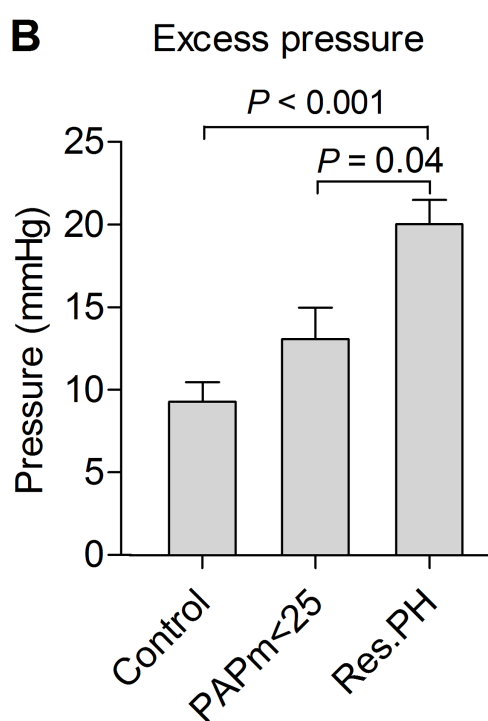
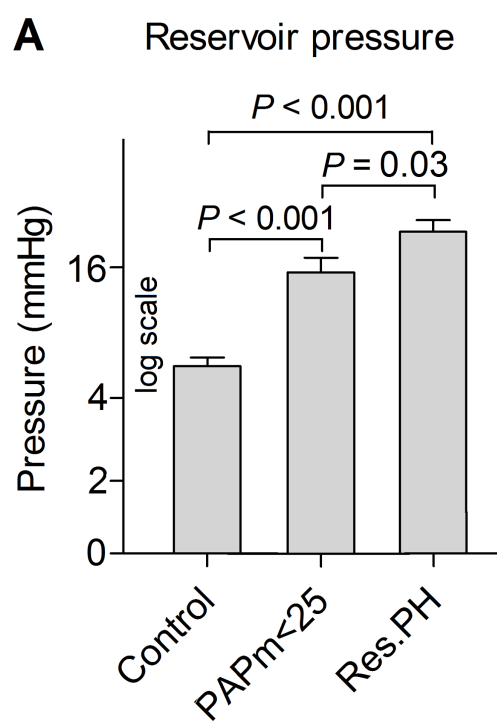
901
902

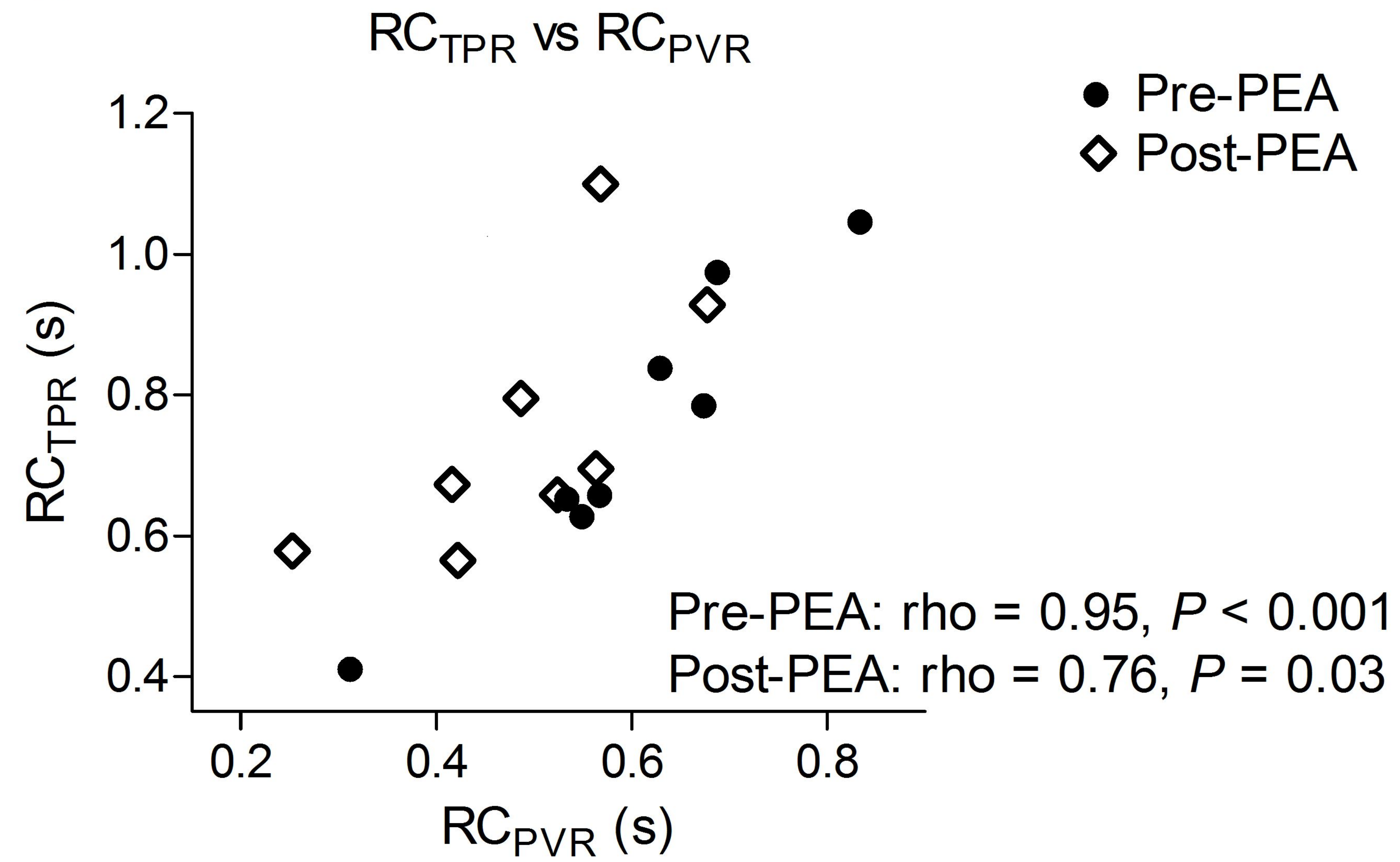
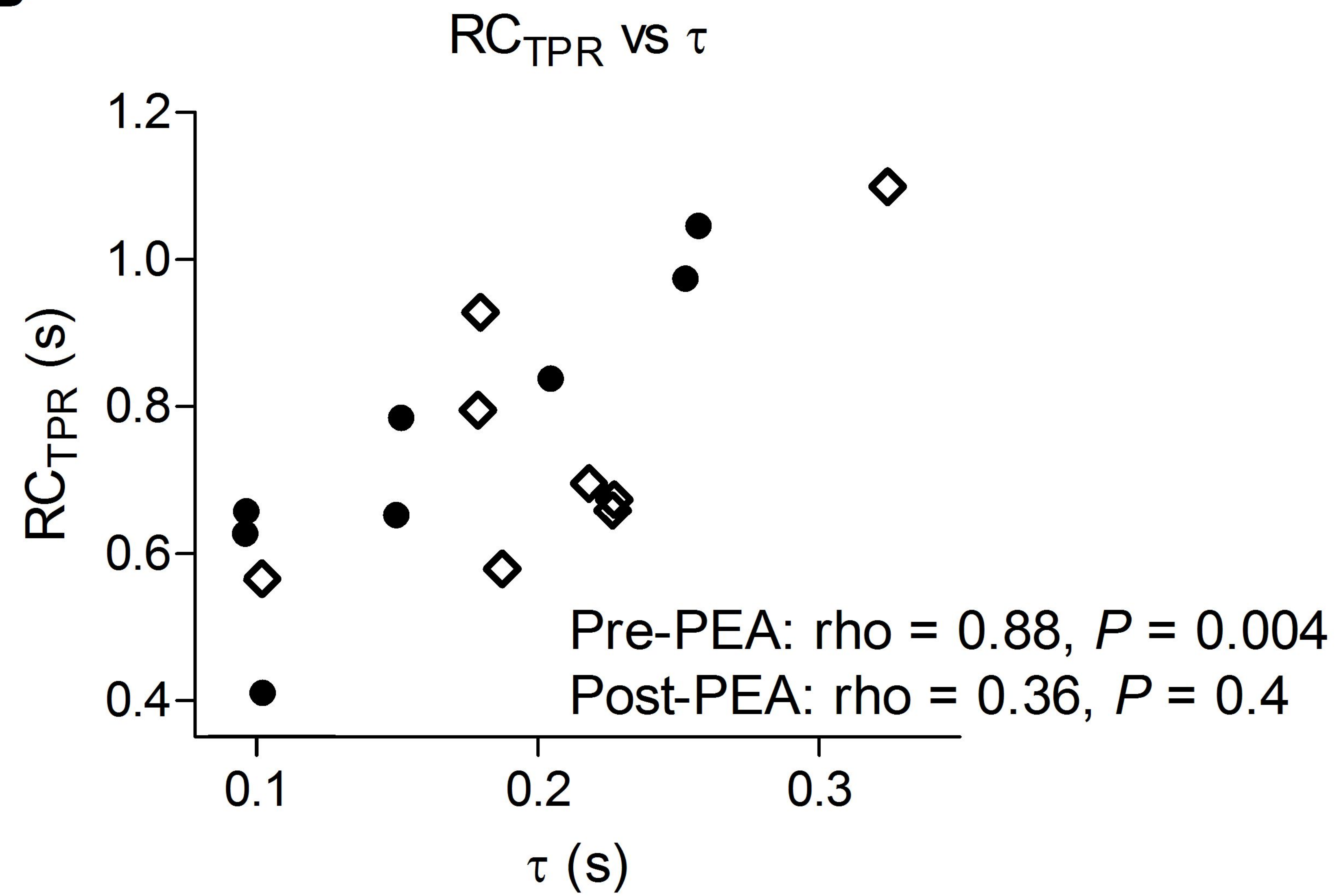










A**B****C**